University of Stavanger

Faculty of Science and Technology

MASTER'S THESIS

Study program/ Specialization: Petroleum Technology, Production Specialization	Spring semester, 2012..... Open
Writer: Magnus Palm	…… (Writer's signature)
Faculty supervisor: Thor Martin Svartås	
Titel of thesis: The effect of some hydrocarbon liquids on methane hydrate nucleation	
Credits (ECTS): 30	
Key words: Clathrate Hydrates, Nucleation, Methane, Alkanes, Nucleation, Arrhenius plot Surface tension	Pages: ……46…… + enclosure: ……6…… Stavanger, …15/6 2012…….. Date/year

Preface

I wish to thank the supervisor Thor Martin Svartås, for always being available and showing true interest in the progress and content of this thesis.

I also wish to thank Ke Wei and Eirik Høvring for valuable input and interesting discussions, and last but not least, the staff at the laboratory and library of UiS.

Legend

P	absolute pressure, bar
P	probability
T	absolute temperature, °C, K
T_{eq}	hydrate equilibrium temperature, °C
ΔT	subcooling temperature, °C
t	time, min
td	time of hydrate detection, time counted from start of stirring, min
h	hour
J	the rate of nucleation, $m^{-2}s^{-1}$ if assuming HEN, $m^{-3}s^{-1}$ if assuming HON
τ	offset from t = 0 of estimated p = 0, min
p	cumulative probability of detecting hydrate formation at a certain t
n	the size of a cluster, referring to the number of basic units included in the structure
N	a certain number of supercritical nuclei
HON	homogeneous nucleation
HEN	heterogeneous nucleation
STP	standard pressure (1 atm) and temperature (25 °C)
σ	surface tension, mN/m
σ_w	interfacial tension between water and liquid or gaseous hydrocarbon, mN/m
ΔG	Gibbs free energy of a hydrate cluster, J
ΔG_v	Gibbs free energy of the surface of a hydrate cluster, J
Δg_v	Gibbs free energy change per unit volume of hydrate bulk phase, J

E_A	Activation energy of nucleation, J
k_B	Boltzmann's constant, J/K
LHC	liquid hydrocarbon component
sI	structure I hydrate
sH	structure H hydrate
sII	structure II hydrate

Abstract

The effect of some liquid hydrocarbon components on the nucleation process of methane clathrate hydrate has been investigated during isochoric, constant temperature nucleation experiments.

The detected nucleation times were analyzed statistically and the key properties of nucleations were estimated through regression

Most of the investigated components had a delaying effect on the nucleation, but with little difference between the components. This was the case for iso-pentane, n-hexane, n-octane, pentyl-benzene and n-dodecane.

n-pentane showed virtually no effect, while cyclohexane had a nucleation propagating effect, though this may be because it can form a different hydrate structure (sII). Melting point tests indicated the formation of both sII and sI in the system when cyclo-hexane was present.

The experimental results showed generally low reliability and it was concluded that this was because of the highly stochastic nature of the investigated phenomenon combined with statistical analysis on too little data.

A novel method of detecting hydrate formation was used: a small but distinct pressure pulse was the first sign of hydrate formation, and this was successfully utilized to identify the time of hydrate formation in all the experiments.

The activation energy of stable hydrate nuclei formation was successfully calculated using the Arrhenius plot method, and this could be used to calculate the critical radius of 31,8 Å.

Table of Contents

Introduction

Clathrate hydrates of gases was regarded as a curiosity, until it was found to cause problems with transport of natural gas in pipelines [1, 2]. Later, it has also gained interest because there is evidence of very large natural deposits of mostly methane hydrate. This is seen both as a possible energy source, a threat to climate because of methane being a greenhouse gas, and a possibility to store CO_2 permanently as deep-sea hydrate deposit. [2]

Hydrates have an ice-like structure and appearance, but unlike ice it can form at temperatures far above 0 °C, at pressures relevant to gas and oil production[2, 3]. If this is not avoided, hydrates may plug pipes and equipment and cause significant economic losses, because it can be a very difficult and time consuming process to remove the plug. It can also be a severe safety hazard, as a hydrate plug may have higher pressure on one end. If such a plug gets loose from the pipe wall, it may become an accelerating projectile causing potentially deadly damage downstream.[2, 3]

The formation of gas hydrates in the petroleum industry is prevented in a number of ways. Obviously the temperature and pressure can be kept at levels where hydrate is not thermodynamically stable. This is often not practical, and this mostly calls for the use of chemicals to prevent or delay the formation of hydrates.[2, 3]

Gas hydrates resembles ice in that it may be controlled by the same kind of chemicals that suppress the freezing-point thermodynamically, like alcohols. Methanol and glycols have been extensively used historically. While this method certainly can solve the problem, it may also be very costly because the amount of chemicals can be very high, up to 50 wt% (based on the water content of the stream). Additionally, methanol is a poisonous and highly flammable substance, and can therefore pose serious handling risks. [2, 4]

The development of low-dosage hydrate inhibitors in the last two decades have therefore achieved great attention, as it can allow the amount of chemicals used to be much lower, usually between 0.1 – 1.0 wt% active ingredient. Low-dosage hydrate inhibitors are divided into two groups based on their actions: kinetic inhibitors (KHIs) and anti-agglomerants (AAs).[4]

Because hydrates is a solid phase that crystallizes in an aqueous solution, nucleation of the solid phase must preceed crystal growth. KHIs work mostly in that it disturbs the nucleation

process, although they also have slowing effects on crystal growth [4], although it has been reported that one of the most utilized KHIs, PVCap, may actually promote hydrate nucleation if present at very low concentrations [5].

AAs works differently in that they prevents the agglomeration of hydrate crystals into lumps that can plug the pipes, thus the hydrates become transportable in the oil well stream and poses less problems to production. AAs may perform better at high subcooling temperature (temperature decrement below the limit at which hydrates are thermodynamically stable, in effect the melting point). However, AAs don't work well if the water content increases above ca 50%, as the flow may become too viscous. [4]

Because the main aim of KHIs is to delay nucleation, this phenomenon is of great interest to investigate. Unfortunately, the phenomenon appears to be very complex and there is still considerable need for extending the knowledge base on the subject. The stochastic, non-macroscopic and high-pressure nature of the phenomenon makes experimental research on the subject challenging and time-consuming. [5-7]

One part of the problem that may have great impact of the knowledge application on real world problems is that the petroleum production is dealing with well streams composed of a large number of hydrocarbon components, rather than just a minimalistic binary system of water and gas. Other components, such as liquid hydrocarbons, may take active or passive part of the nucleation and hydrate forming process, and this is one of the areas where knowledge needs to be expanded.[6, 8, 9]

Hydrocarbon liquids may have at least three different effects on a hydrate forming system of water and gas:

- It may take part in the hydrate structure as guest together with the gas molecules [7, 10, 11]
- It may act as a transport barrier between the gas and the water phase [6]
- An oil film may alter the surface tension between water and gas phase [12-14]

Defining the Thesis

In a previous work in an unpublished bachelor's thesis by Nordbø [15], it was indicated that hydrocarbon liquids had an promoting effect on the nucleation of methane hydrate detection. Furthermore, her results indicated that this effect may be related to the molecular size of the hydrocarbon liquids, apart from the interfacial tension.

This work was intended to be a further investigation on this subject.

Because of the mutual solubility of hydrocarbon fluids, the composition of both the liquid and the gas hydrocarbon phase may be altered at high pressures [6, 16]. A different composition of the gas phase will in itself alter the hydrate formation properties of a system [17] and to minimize this effect, pure methane gas was selected instead of a more realistic multiple component gas composition.

Nordbø [15] used a method of constant cooling of an isochoric system, and the cooling was continued until the system responded with hydrate formation. In this work, the method was to keep the pressure and the temperature constant at a certain subcooling, to let the system respond without being forced to do so by an ever-increasing level of subcooling.

Theory

Hydrate formation is usually described as a form of crystallization and consists of "nucleation" and "growth" phases. During primary nucleation, nuclei of the new phase are generated in a supersaturated aqueous solution. The nucleation process ends when stable nuclei above a certain critical size appear, which will then continue to grow into macroscopic crystals in the growth phase. Those supercritical nuclei have a large probability of monotonic growth, instead of oscillating size in the supersaturated solution. [18]

Nucleation

Because nucleation is a stochastic process, it may be beneficial to think of it in terms of statistics and probability. In general, the probability P of generating a certain number N of supercritical nuclei in a nucleation process at constant physical conditions can be schematically described by Fig. 1.

Here, point A marks the start of a static super-saturation. Point B annotates the time at which there is a probability $P > 0$ to form the first nucleus above critical size, and point C is the time after which we have steady state nucleation. [19]

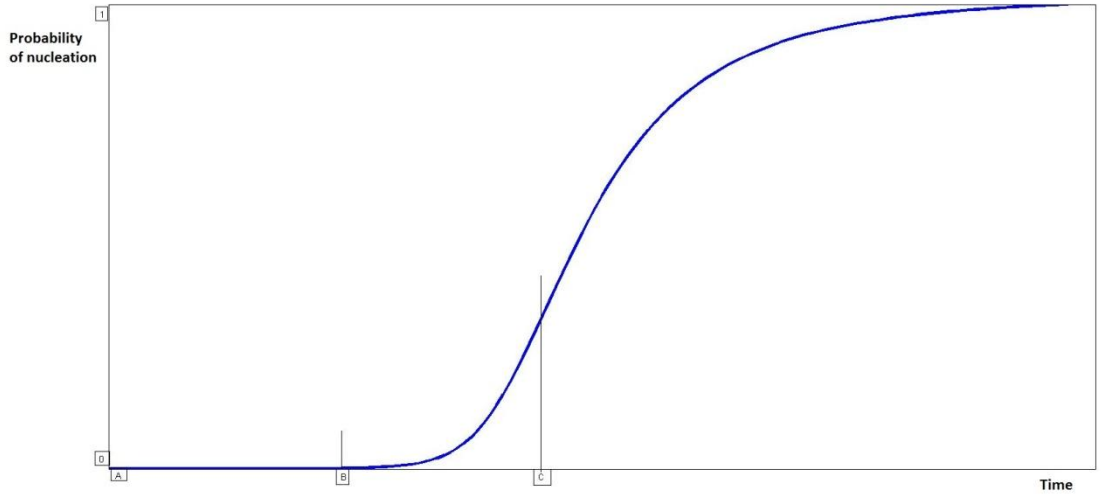

Fig. 1, schematic depiction of the nucleation process

A challenge when approaching the scientific literature on the subject is that the terminology is far from consistent. Different terms are used to describe the different depicted in Fig. 1, possibly because in many cases two or three of the points A, B and C in practice coincides in time. Additionally, the same words are also sometimes used to describe features of a *single* nucleation event, which may add to the confusion.

I will in the following try to give a short review of the terms used in the literature referred to in this thesis.

Lag time, time-lag

Sloan and Koh [17] appear to use this term somewhat inconsistently. On page 114 they state that it is the time between nucleation first occurs until it can be detected by macroscopical instruments. Later, at page 121 and 139, they use it to denote the time period A-B in Fig. 1.

Kashchiev [19] and Toschev et al [20] use lag time, which they denote τ, to denote the transient time period B-C in Fig. 1.

Abay [5] also apparently use the term inconsistently. On page 4 he states that it is the time between the existence of the first supercritical size nucleus until it can be detected by the equipment used in his experiments, but on page 27 he uses the term to describe the time period A-B in Fig. 1. On page 57 he state that it is the time B-C of Fig. 1. His description is only consistent if the transient period of the nucleation process is in fact the time before the occurance of nonzero probability of detection of supercritical nucleus.

Induction time

Abay [5] uses this term to denote the time period between the physical onset of the experiment until supercritical nucleation is first confirmed. The term is used for *a single* experiment, and can therefore vary considerably.

Sloan and Koh [17] use the same definition, but explicitly state that induction time includes a metastable period without any supercritical nuclei, and a certain time period where supercritical nuclei exist undetected by the experimental equipment. On page 114 they state

that the induction time is most likely dominated by the metastable period, and not the period in which supercritical nuclei remain undetected.

Kashchiev [21] also agrees with this definition, and point out that depending on the experimental technique used, the induction time ends by either one single detectable nucleus or a large number of nuclei (if the nuclei are detectable only in large numbers).

Natarajan et al [18] also uses induction time to denote the metastable period, before stable nuclei have formed.

Toschev et al [20] uses "induction time" to describe the transient period. Because of the nature of their experiments, this corresponds to period A-C of Fig. 1.

Tegze et al [22] uses "induction time" in exactly the same way as Toschev et al [20], but make the important note that because of the low viscosity of an aqueous solution, the transient period of hydrate nucleation process is very short, calculated to less than 1 ns, and therefore often negligible.

Transient period

Toschev et al [20] states that the transient period is the time before the nucleation rate has reached steady state, A-C in Fig. 1. They clearly say that if there is a significant transient period in a nucleation process, the cumulative distribution function of the probability of nucleation will have a visible sigmoidal shape ("s-shape"). Further, they point out that the number of experiments needed is very large, if one wishes to calculate the rate of nucleation as well as the length of the transient period. In their work they did 500 repetitions of each experiment.

Kaschiev [19] explains that the transient period is when the concentration of clusters of subritical size n changes with time, n being the number of building blocks. So, during the transient period of the nucleation process, the size distribution of the subcritical clusters is not constant.

Steady state period

After a steady, time-independent size-distribution of subcritically sized cluster has been established, the nucleation process is said to be stationary, or steady state. [19]

During steady state nucleation, the probability of not detecting a certain number of supercritical nuclei has a steady half-life, that is the same as saying that the cumulative distribution function of the probability has reached a hyperbolic behavior. [20]

Detection of one nucleus, or many?

Kashchiev [21] points out that depending on which experimental system that is examined, the detection of supercritical nucleation is detected will not always refer to the detection of the (single) first nucleus formed. In some systems the end of the metastable state will be at the appearance of a great number of super-critical nuclei.

When it comes to hydrate nucleation in a relatively large sample container, it is interesting to note that turbidity experiments performed by Natarajan et al [18] led them to the conclusion that the detection of nucleation were indeed the detection of a very large amount of nuclei. In addition, they observed a very sudden change in turbidity from clear to translucent. This led them conclude that it is unlikely with a long period of time in which supercritical nuclei existed undetected. This is also indicated by other observations coinciding with the turbidity change, for example a slight dip in reactor pressure as well as a sharp increase in gas consumption (they maintained a constant gas pressure in a stirred container at constant pressure).

Nomenclature in this work

Because of the great inconsistency with respect to terminology, it is needed to explain the terminology used in this work:

"Start" is the start of an experiment, when stirring is turned on after the cooling and relaxation period.

"Time of hydrate detection", or "t", is counted from t_{start} = 0 min.

"Offset", or "τ", is assumed to be a time lag between the appearance of supercritical nuclei and the detection thereof. In this work τ is estimated using statistical analysis of a series of experiments. It is used and estimated in accordance with the method described in [5, 23, 24].

"Rate", or "J", is the stationary nucleation rate, the average number of stable, supercritical nuclei formed per unit time and unit volume in a solution at a constant subcooling

temperature. It is used and estimated statistically from a series of experiments in accordance with the method described in [5, 23, 24].

Theoretical description of the statistical method used in this work

This part is written in accordance with Abay [5], Jiang and ter Horst [23], and Takeya et al [24].

At a constant supersaturation, the generation of stable nuclei is described as a random process where a large amount of subcritically sized clusters fluctuate in size, and some of these clusters eventually grow to supercritical size, reach a state of monotonic growth and are detected.

If the appearances of detectable nuclei are independent events, the probability P_m of forming m nuclei in a time interval is described by the Poisson distribution:

$$P_m = \frac{N^m}{m!} e^{-N} \qquad (1)$$

where N is the average number of nuclei that appear in the time interval. If $m = 0$,

$$P_0 = e^{-N} \qquad (2)$$

If we assume that we detect nucleation if at least one supercritical nucleus is formed, it is interesting to define the probability of formation of at least one such nucleus:

$$P_{\geq 1} = 1 - e^{-N} \qquad (3)$$

Because we assume stationary nucleation, the number of nuclei formed in a time interval Δt is

$$N = JV\Delta t \qquad (4)$$

or

$$N = JA\Delta t \qquad (5)$$

depending on whether we have homogeneous or heterogeneous nucleation. V is then the volume of the sample and A is the area of the interface where nucleation is taking place.

Logically, one can exclude volumetric and superficial input when analyzing and comparing experiments, if the volume or area is identical in all experiments. We can then define the probability of forming at least one supercritical nucleus in a time period from start as

$$P_{\geq 1} = 1 - e^{-Jt} \qquad (6)$$

The above formulas refer to the *formation* of nuclei. If there is a certain time delay between the formation and the *detection* of supercritical nuclei, it is possible to assume stationary nucleation (formation) from start, and still have an offset time relative to start, which then mark the end of a period where the probability of hydrate detection is zero[1]. We then denote $P = P_{\geq 1}$ as $P(t)$, the formation-detection time delay as τ, let t be the time of hydrate detection and we may write

$$P(t) = 1 - e^{-J(t-\tau)} \qquad (7)$$

Equation (7) can be regarded as a cumulative distribution function describing the probability of detecting hydrate nucleation at or before a certain time t_d.

Because equation (7) is a probability function, a series of experimentally measured values of t_d can be used to estimate the parameters of the function itself, namely J and τ.

This is made utilizing the following formula as an estimator for P(t)

$$P = \frac{M^+(t)}{M} \qquad (8)$$

where M is the total number of experiment in the series, and $M^+(t)$ is the number of experiments where t_d was registered at a certain time t.

From a $P - t$ plot, the parameters J and τ may then be estimated through curve-fitting.

[1] Note that Abay [5] writes that the steady state nucleation regime starts at $t = \tau$. This is probably an not correct since he acknowledges eq. (4) above, which demands steady state regime from start. In this work the τ time lapse is assumed to be part of the steady state nucleation period, and that the true transient time period is negligible in accordance with Tegze et al [22].

Driving force, subcooling

The hydrate structure is generally thermodymically favoured at low temperatures and high pressures[2, 5, 6, 25]. At a certain pressure, hydrate phase is only thermodynamically stable at temperatures below a certain equilibrium temperature, T_{eq}. A system without supercritical hydrate nuclei may be cooled below this temperature without immediate (detectable) formation of hydrate nuclei or crystals and it is said to be in a metastable state until the spontaneous formation of hydrate nuclei, which then grow to stable crystals. During metastability, the temperature difference between T_{eq} and the temperature at hand is termed the subcooling temperature ΔT.

Apart from this, agitation is also an important factor and promotes nucleation of a system which is in metastable condition.[17, 26]

Surface tension

The surface tension and interfacial energies of a system may be an important factor of the hydrate formation [27], and the surface tension between water and hydrate is a part of the critical radius formula of the classical nucleation theory[28]:

$$r_c = -2\sigma/\Delta g_v \qquad (9)$$

where r_c is the critical radius of a thermodynamically stable nucleus, σ is the surface tension between the hydrate phase and the liquid water, and Δg_v is the free energy change per unit volume (of the hydrate phase).

Because we most likely have heterogeneous nucleation [5, 17], the surface tension between the water and the hydrocarbon gas/ liquid phase may also be an important factor.

Firoozabadi and Ramey [29] have developed a correlation (Fig. 2) for calculating the surface tension between water and any kind of non-polar gaseous or liquid hydrocarbon, and this gives a possibility to estimate the surface tension at pressures and temperatures which may be hard to find listed in the literature. The correlation is developed from experimental data and allows the interfacial tension to be calculated from input of water and hydrocarbon densities and reduced temperature of the hydrocarbon component.

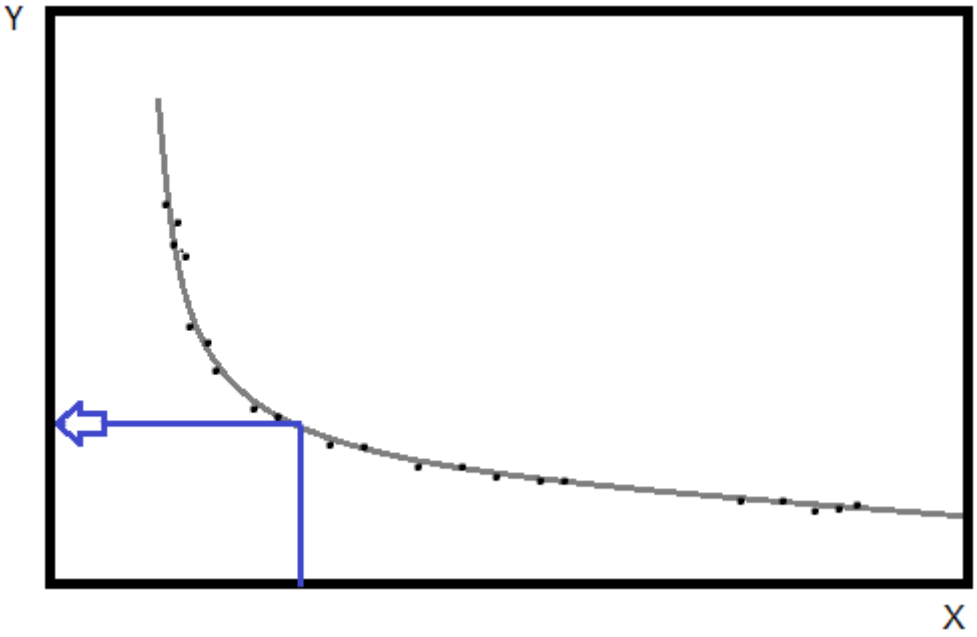

Fig. 2, description of the Firoozabadi and Ramey correlation, and how to use it [29]

The x-axis of Fig. 2 is $\Delta\rho$ and the y-axis is $(\sigma^{0,25} \times {T_r}^{0.3125})/\Delta\rho$, where $\Delta\rho$ is the density difference between water and the hydrocarbon at experimental conditions, in g / cm^3, σ is the interfacial tension between water and hydrocarbon, T_r is the reduced temperature $\frac{T}{T_{crit}}$ and the curve is fitted from experimental results featuring several different hydrocarbons. The correlation can be used to estimate the surface tension since all other variables are either known or tabulated.

In Table 1, the hydrocarbon-water interfacial tension σ_w was estimated from [29] at experimental conditions, and compared with literature data referring to near standard conditions (25 °C, 1 atm). The densities and critical temperatures of the hydrocarbons were calculated using PVTsim v 20.

It should be noted that according to Firoozabadi and Ramey [29], the surface tension is expected to increase with the following factors:

- decreasing temperature

- increasing pressure in the case of methane

-decreasing pressure in the case of hydrocarbon liquids (small effect)

1. The estimations for many of the hydrocarbon liquids in Table 1 therefore seem to be too low compared to the experimental values obtained at much higher temperatures.

Table 1, some experimental and calculated values of σ_w

hydrocarbon component	**σ_w, experimental, [mN/m]**	**$\sigma_w$estimated from [29], 90 bar, [mN/m]**
methane (gas)	25 °C, 90 bar: 63.5 [30]	6 °C - 7 °C - 8 °C: 64.8 – 64.6 – 64.6
n-pentane	26.3 °C, 1 atm: 48.71 [31]	6 °C - 7 °C - 8 °C: 38.5 – 38.8 – 39.0
iso-pentane	25 °C, 1 atm: 50.1 [12]	6 °C - 7 °C - 8 °C: 36.5 – 36.8 – 37.0
n-hexane	30 °C, 1 atm: 51.1 [32] 6 °C - 7 °C - 8 °C, 1 atm: 51.9 - 51.8 – 51.7 [33][1]	6 °C - 7 °C - 8 °C: 50.3 – 50.6 – 50.9
cyclo-hexane	30 °C, 1 atm: 51.4 [32]	6 °C - 7 °C - 8 °C: 41.1 – 41.4 – 41.9
n-octane	30 °C, 1 atm: 50.8 [32] 6 °C - 7 °C - 8 °C, 1 atm: 52.9 - 52.8 – 52.7 [33]	6 °C - 7 °C - 8 °C: 48.9 – 49.1 – 49.4
pentyl-benzene[2]	30 °C, 1 atm: 40.6 [32]	6 °C - 7 °C - 8 °C: 41.4 – 41.2 – 41.0
n-dodecane	6 °C - 7 °C - 8 °C, 1 atm: 53.85 - 53.8 – 53.75 [33]	6 °C - 7 °C - 8 °C: 52.6 – 52.8 – 53.0

[1] Values were extrapolated graphically

[2]PVTsim v 20 did not provide calculation for pentyl-benzene. In this case it was used STP density and critical temperature data from www.wolframalpha.com were used.

Activation energy

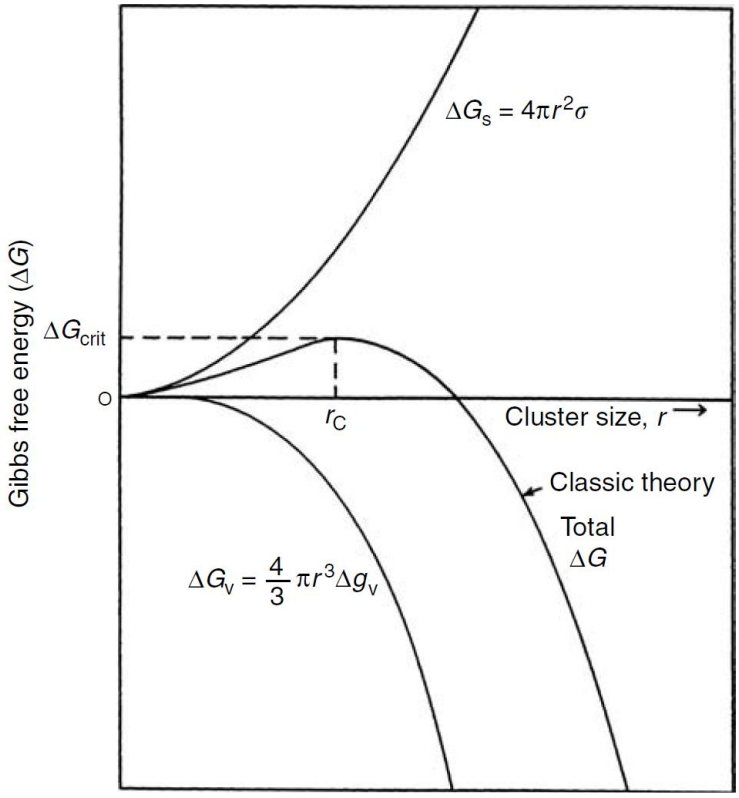

Fig. 3, conceptual picture of activation energy of stable nucleus [17]

The formation of a stable solid hydrate nucleus in a supersaturated solution may be described by classical nucleation theory where the Gibbs free energy ΔG of the solid particle formed is dependent of both the increasing free energy of the particle surface, ΔG_s, and the decreasing free energy of the bulk, ΔG_v:

$$\Delta G = \Delta G_s + \Delta G_v = 4\pi r^2\sigma + \frac{4}{3}\pi r^3 \Delta g_v \quad (10)$$

The saddle point of Fig. 3 represents the activation energy E_A of the formation of stable nuclei in a subcooled metastable hydrate solution system [17, 34], and as such we expect it to be described by the Arrhenius formula[35]:

$$J = J_0 \exp\left(\frac{-\Delta G}{k_B T}\right) \quad (11)$$

where J is the rate of nucleation, J_0 is a (constant) pre-exponential factor, k_B is Boltzmann's constant and T is absolute temperature. Because of this, it is possible to evaluate the

activation energy from an Arrhenius plot analogous to the method described by Schmitt et al [36]. Schmitt et al also describes the possibility to find activation energy for the two different reactions nucleation and growth. This is also analogous to the hydrate formation. To find the activation energy for nucleation, the nucleation rate J should be used. To find the activation energy for growth (negative, since it is an exotherm reation), the growth rate should be used[6, 36].

It follows from Eq. (11) that a plot of ln (J) vs $\frac{1}{T}$ for values of J found experimentally at different temperatures T should form a straight line where the slope is the activation energy.

Homogeneous and heterogeneous nucleation

Homogeneous nucleation is the formation of the new, solid hydrate in an aqueaous solution super-saturated with gas molecules. It is very unlikely to occur in real cases, because the ΔG_s part of Eq. (10) is larger than if the nucleation occurs at another surface instead. This surface could be the surface of the container wall, some solid dispersed contamination an existing ice or hydrate particle, or the interface of the water and the gas phase. This interface is often the most favourable site of nucleation, not only because it is favourable because of less ΔG_s, but also since it is likely to have the largest saturation of gas molecules. [17, 37]

If it is assumed that nucleation occurs at or immediately close to the water- gas interface, J of Eq. (10) will have the unit $m^{-2}s^{-1}$ instead of $m^{-3}s^{-1}$. [37]

Different hydrate structures

Hydrates are solid phase structures where water molecules form cavities, which are not stable if they are empty. There are three common types of structures, sI, sII and sH, and these are ideally constructed from five different cavities made up of hydrogen-bonded water molecules.

The structures of the different cavities are showed in Fig. 4. The cages are commonly named after the surrounding facets, referring to Fig. 4: A = (5^{12}), B = ($5^{12}6^2$), C = ($5^{12}6^4$), D=($4^35^66^3$), E = ($5^{12}6^8$). [38]

The cages vary in size, with radius from 3.95 – 5.79 Å, depending on which cavity. Because they have different size, they need to be stabilized by guest molecules of different size – this is the reason why different gas compounds stabilize different hydrate structures. Which

structure of hydrate that will form in a system will therefore depend on which hydrate formers (guest molecules) that are present, and in which ratio.

Generally, the guest molecules should be non-polar and must not be able to form hydrogen bonds with the water molecules.[38]

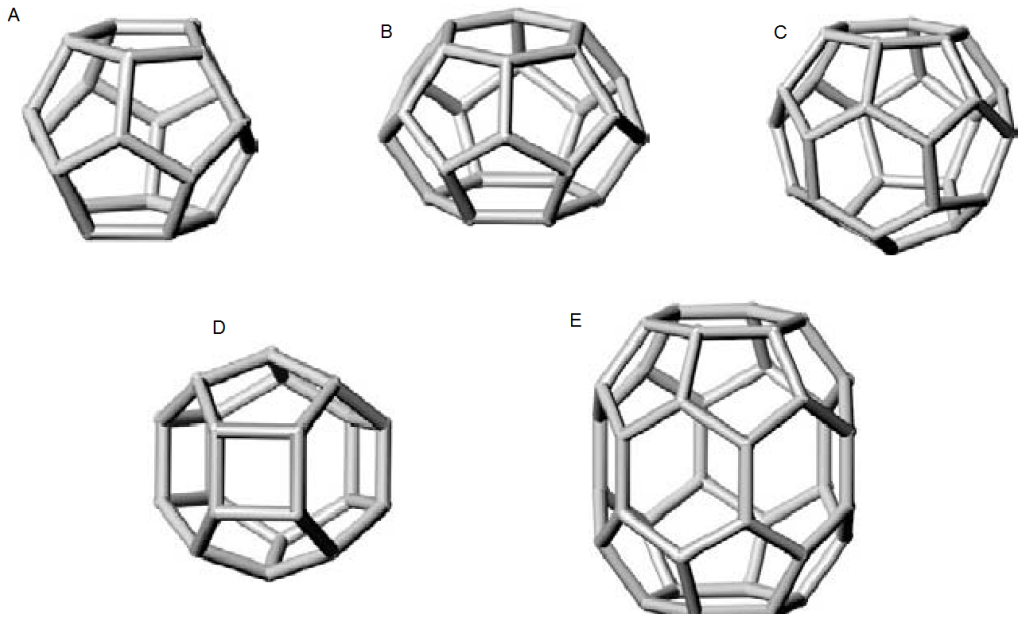

Fig. 4, the cavities of clathrate hydrates, [38]

In systems where methane is the only available guest molecule, the thermodynamically preferred hydrate structure is sI at moderate pressures. However, if guest molecules that can fill the larger cavities of structure II or sH are present, those structures may form instead of sI. [17]

Because the focus of this work is to investigate the effect of liquid hydrocarbon component on methane sI hydrate nucleation, it is of great importance to know that both cyclo-hexane, iso-pentane, n-pentane, n-hexane has been reported to form sII or sH, either with methane alone or as co-guests with other hydrate formers.

Lee et al reports that n-pentane and n-hexane can enter the large cages of sH-hydrate as co-guest together with 2-2-dimethylbutane [39], but it is not reported to form hydrate with methane alone [17, 39]. CSMgen, is a hydrate equilibrium calculation program distributed with Sloan and Koh [17]. This program calculates that a methane – water system with n-

pentane and n-hexane will still nucleate as sI hydrate, but this will form at a temperature ca 4.2 °C lower than with a pure water – methane system.

Mehta et al [7] reports about iso-pentane and methane forming sH hydrate, and CSMgen calculate that an iso-pentane – methane – water system will nucleate as sH, not sI, though at lower temperatures at a given pressure compared to the pure methane sI hydrate.

Cyclo-hexane is reported to form sII hydrate together with methane [11].

Walsh et al [40] report from molecular dynamics simulation project of pure methane hydrate nucleation, which results in a combination of sI and sII bonded by non-standard structural cages. Because this describes the very first event of nucleation, it indicates that it does not necessarily have to be only one, uniform structure that forms at nucleation.

Experimental Section

Experimental setup

The experiments were performed in accordance with the work of Abay, using the same type of equipment and procedure as described in his PhD Thesis [5]. The experimental setup is schematically shown in Fig. 1.

The setup included a tailor made constant-volume titanium cell with magnetic stirring. The temperature was regulated using water circulated through a cooling cap. The temperature was measured using a 1/10 DIN Pt100 element of accuracy 0.03 °C, and the absolute pressure was measured using a Rosemount 3051 TA. The accuracy of the transmitted temperature and pressure signals were ± 0.1 °C and ± 0.2 bar, respectively [5].

The temperature regulating equipment used was a Julabo F34 HL with programming feature and a temperature stability of ± 0.01 °C. The magnetic stirrer was calibrated to 425 RPM. Because the stirring rate can affect the time of metastability [17, 26], the stirring rate in all experiments were kept constant.

LabView was used to log pressure and temperature data. The data was first analyzed graphically using KaleidaGraph 4.0 and with the assumption of the experimental probability function Eq. (7), the experimental values were fitted to the this function using MatLab 7.11.0.

Limits of thermodynamical stability at defined system conditions, were calculated using CSMGem.

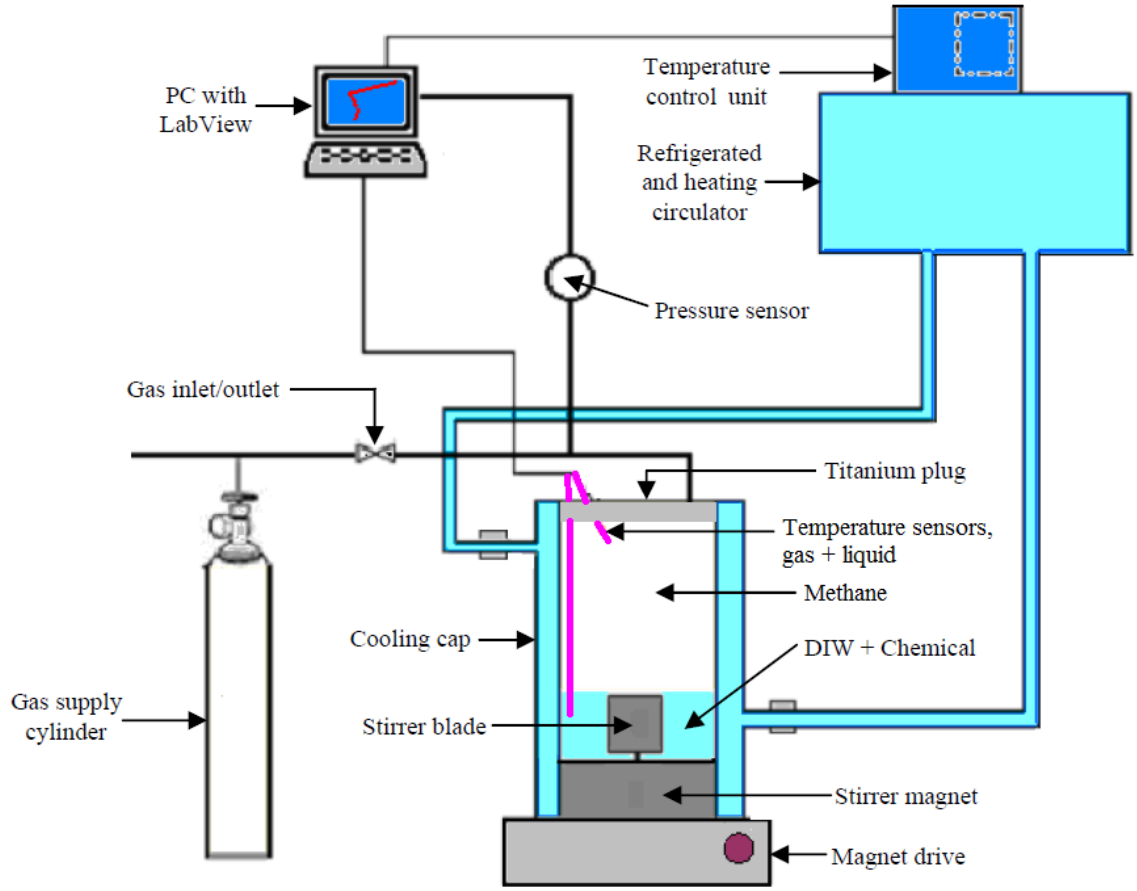

Fig. 5, experimental setup. Modified from [5]

Experimental procedure

Before each experiment the cell was washed twice using tap water, distilled water and dry air. When changing the additive (liquid hydrocarbon), or else when suspecting contamination, dish-washing detergent and / or acetone were additionally utilized. Special attention was paid to the combined gas inlet/ outlet tubing, due to high possibility of finding liquid residues within the tubing close to the cell connection.

Small amounts of high vacuum silicone grease and copper paste were used on the rubber o-rings and the threads, respectively.

To avoid memory effects due to water from melted hydrate [17, 24, 25, 41], the cell was filled with 50 ml of fresh distilled water and 2-6 ml of the liquid hydrocarbon of interest, assembled and purged twice with methane gas at 40 bar during stirring. The methane gas was of purity 5.5 (i.e. 99.9995 mol%). During purging the cell was stirred for a while having reached 40 bars. Stirring was stopped when the cell was depressurized to avoid liquid droplets of water or HC liquid to be thrown towards the cell outlet. Having reached ambient pressure after complete depressurization, the stirrer was restarted to remove residues of supersaturated gas in the liquid phases. It is assumed that equilibrium was reached with respect to the methane/air mix in the liquid phases during the purging process – both during stirring at 40 bar and finally at ambient pressure. After purging, the gas pressure was increased to around 93 bar, which corresponded to a final experiment pressure of 90 bar at the desired experimental temperature. Therefore, the final air residual mole fraction in the gas phase during the experiment is assumed to be less than $\frac{1}{40} \times \frac{1}{40} \times \frac{1}{93} \approx 7 \times 10^{-6}$, which is considered negligible. It may be argued [5] that the last pressurization up to ca 93 bar is not part of the purging process, and should therefore not be counted. While it is true that the final pressurization does not remove any air content from the cell in absolute numbers, it certainly does decrease the stoichiometric mixture fraction of air in the autoclave during the experiment to a value of less than 7×10^{-6}.

The temperature was initially set to be 13.5 °C, which is calculated to be outside the hydrate area for pressure up to 107 bars at the baseline mixture of water and methane.

The temperature was set to 13.5 °C during purging and filling, which is calculated to be outside the methane hydrate region for pressure up to 107 bars.

After a relaxation time of 10 minutes without stirring, the container was cooled at a rate of 3°C/h from 13.5 °C and down to the desired experimental temperature. Having reached the desired bath temperature, the system was allowed to rest for approx. 5 minutes to reach thermal equilibrium in the cell. After this relaxation period, agitation was started and temperature kept constant until hydrate formation was detected.

A novel method was used to find the key time parameters of the experiments; the starting time and the time of hydrate detection. On a plot of pressure vs. time, there was a slight rise in pressure both at start of stirring (which was regarded as the start of the experiment) and also approx. 6 to 12 seconds before the first detection of hydrates by pressure drop in the cell. Thor Martin Svartås, the academic supervisor of this master's thesis, have been working with the experimental setup used for many years. Over time, small but distinct pressure pulses have been noticed to be a consistent feature of every experiment, occurring slightly prior to other signs like temperature rise and gas consumption. The amplitude of the pressure pulse preceding catastrophic growth appears to increase with increasing subcooling, being in the magnitude 10^{-2} – 10^{-1} bar during the present experiments.

It was assumed that the most correct time is measured through these pressure pulses because they are giving the first (quickest) response / sign of process (stirring or hydrate formation). Therefore, these pressure pulses were assumed to be the most accurate, available method of identifying the key time parameters of each experiment [6]. It is worth noting that such pressure pulse was observed to coincide with the sudden change in turbidity at the point of hydrate detection in the experiments by Natarajan et al [18], but they didn't mention using this pulse except as a confirmation of their preferred method of detection.

Experimental analysis

The time of hydrate detection from each experimental series was ranked from shortest to longest, and the cumulative probability of detecting hydrate at $t = td$ were assigned according to Eq. (8).

Curve fitting in MatLab was then used to obtain an experimental estimation of J and τ.

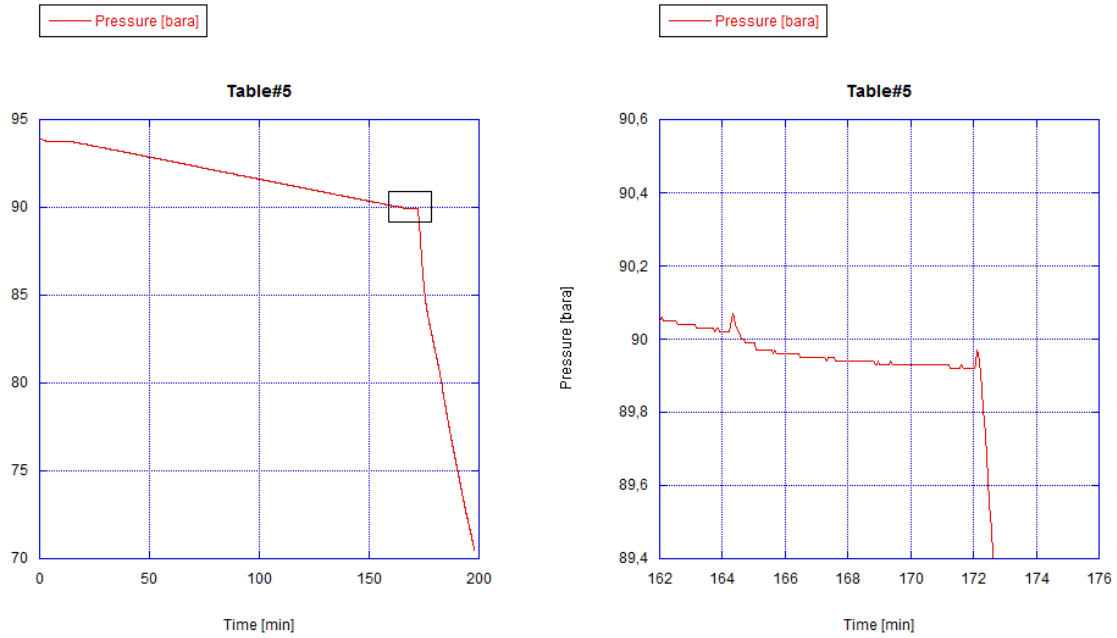

Fig. 6, pressure log of an experiment. Starting point and time of hydrate detection are easily identified.

Results

Baseline series and repair of autoclave

The establishment of water – methane nucleation baseline was the first part of the experimental work. The first six experiments on this baseline were executed at 90 bar and 6 °C, and the measured values of t_d varied between 0.65 – 174.9 minutes, which were considered to be an adequate time range with respect to both the possibility to detect significant effects of additives (on t_d) and with respect to time consumption of the experimental work.

Unfortunately, the threads that connected the magnet holder and the stirring blade were partially broken immediately after conducting the first series of baseline experiments. The equipment were repaired, but to prevent the blade from scraping against the base of the cell interior a thin section (ca 1 mm) of the blade had to be ground off. This was not entirely working adequately and there was still some scraping between the blade and the cell for the next three experiments. The measurements of t_d came on 0.29 – 0.30 min.

A 0.5 mm thick plastic distance disc (nylon) was then introduced beneath the magnet holder ball bearing and the magnet house, and this prevented further scraping. A new series of seven baseline experiments were then conducted, this time the measured values of t_d were between 0.45 – 16.10 min.

This was later combined with a second baseline series that rendered somewhat extended values of t_d, up to 75.9 minutes; nevertheless, it was assumed that nucleation was effected by the repair. The baseline experiments before repair were thus decided not to be used in the direct analysis of the rest of the experiments.

In Fig. 6 the two baseline series before and after repair are plotted in a probability distribution versus time (log scale) plot. A comparison between the two baseline series indicated that the repair was propagating nucleation by shifting the curve towards shorter time for the process to obtain steady state nucleation.

In this and the following $P - t_d$ plots, the t-value of an experiment is the measured time of detection, and the P-value is the probability distribution value calculated using Eq. (8). Because the curve fit used allows negative τ, the probability P to detect nucleation is showed to be above 0 for all $t > 0$.

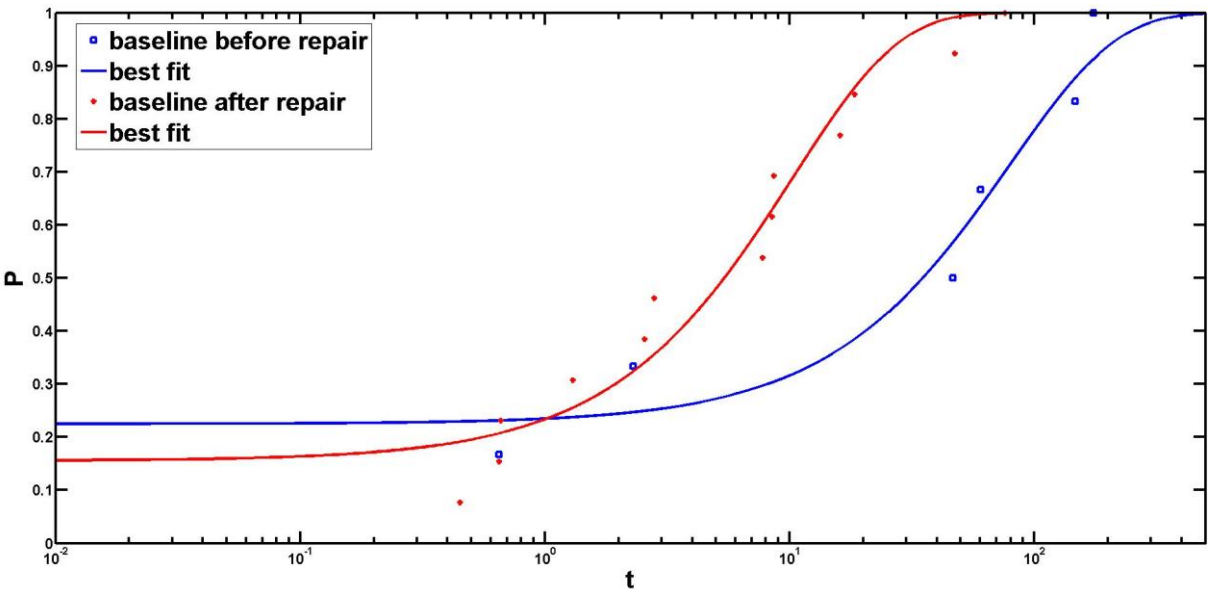

Fig. 7, baseline P-t_d plot before and after repair, 90 bar, 6 °C, ΔT = 6 °C

In the following presentation / discussion, “baseline”, or “baseline 6 °C”, shall refer to the combined series of experiments conducted after the repair as described above, if not otherwise stated.

Due to the relatively short experimental values of t_d retrieved from baseline 6 °C, it was also decided to established a baseline at temperature of 8 °C (subcooling ΔT = 5 °C) to avoid too fast nucleation, and later also a baseline at 7 °C. If subcooling is too low and nucleation occurs too fast after start of stirring there is a probability that nucleation could take place during the non-stirred cooling cycle and “disturb” reliable measurements. Fig. 8 show a $P - t_d$ plot of baseline for 6 °C, 7 °C and 8 °C. This figure shows that at a certain time $t > 0$, the probability to have detected nucleation is increasing as a function of increasing temperature, which is as expected as higher temperature reduce the driving force of nucleation.

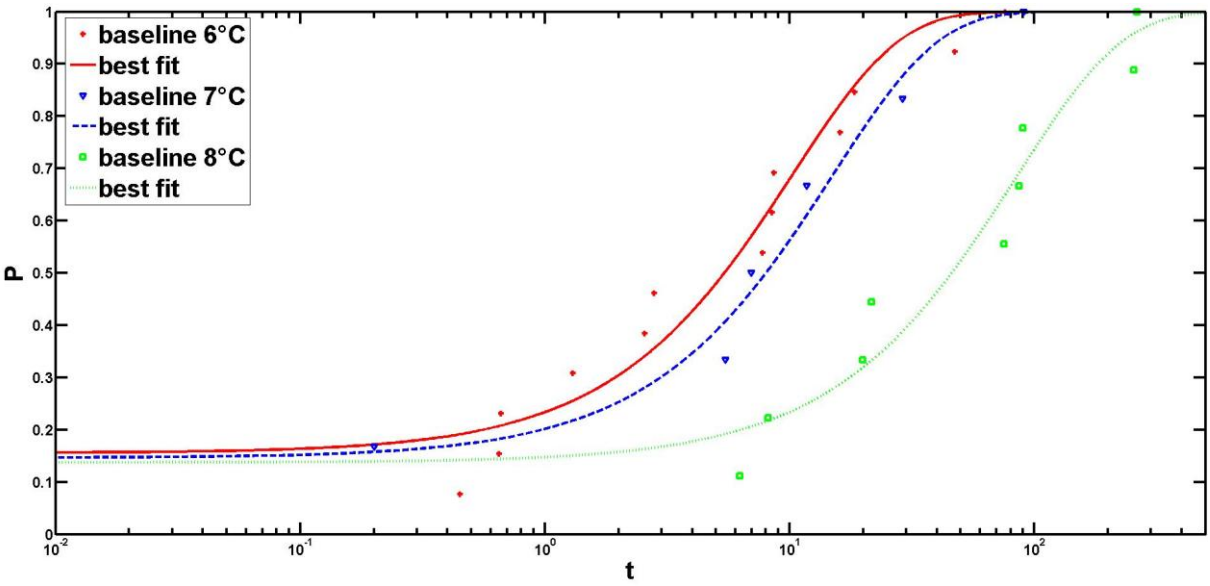

Fig. 8, baseline $P - t_d$, 6 °C, 7 °C, 8 °C, 90 bar

Experiments were then carried out for a number of hydrocarbon liquids, and some variations were executed with respect to temperature and added volume of hydrocarbon liquid. The experimental pressure was always kept at 90 bar, and water volume were always kept at 50 ml.

Table 2, overview of main experiments

Additive	Added volume, ml	Experimental temperature, °C

no additive = baseline	None, only 50 ml distilled water	6, 7, 8
n-pentane	4	6
n-hexane	2	6
n-octane[1]	2	6, 7, 8
n-octane	6	6, 7, 8
n-dodecane	2	6
iso-pentane	4	6
cyclo-hexane	2	6, 8
Pentyl-benzene	2	6

A $P-\mathrm{td}$ plot of the main experiments conducted at 6 °C is shown in Fig. 9.

[1] Several series were done with n-octane 2 ml, 6 °C. If not otherwise stated, "n-octane 2 ml 6 °C" refers to the combined series of all these sets.

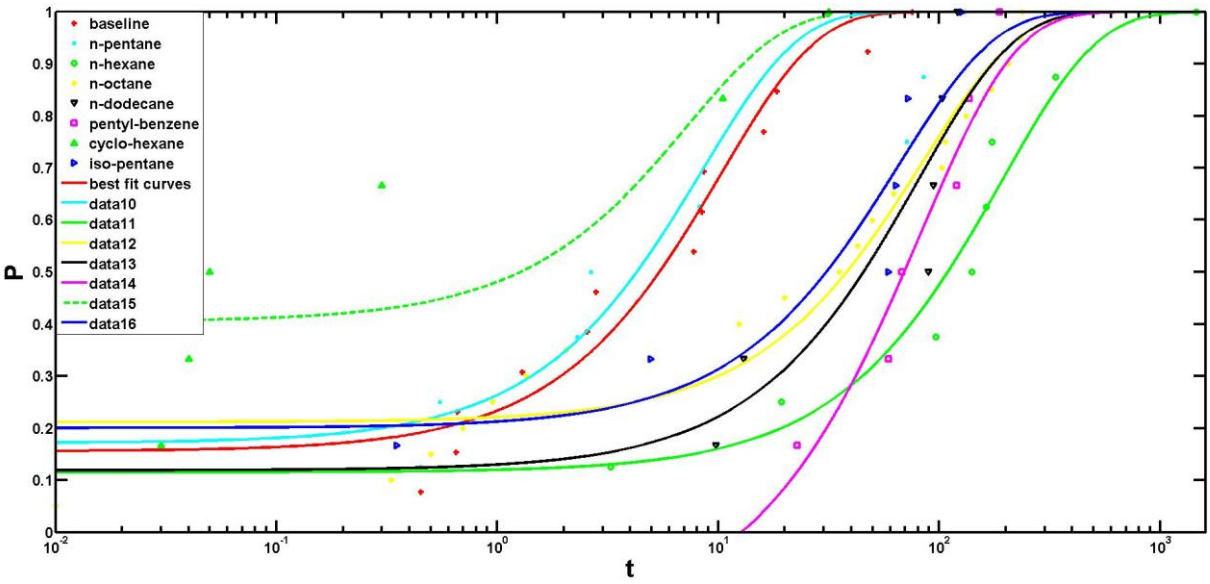

Fig. 9, $P - t_d$ plot of main experiments 6 °C, including baseline, 90 bar

Analyzing and plotting the results, some groups of hydrocarbon liquid appeared to produce results that were part of the same distribution though individual curves could look different at first sight. Fig. 10 shows a plot where the data of iso-pentane, n-hexane, n-octane, n-dodecane have been combined into a group termed “group a”. As demonstrated by the curve fit versus data points support assumption that these points are part of the very same distribution function and that differences, if any, most probably are negligible.

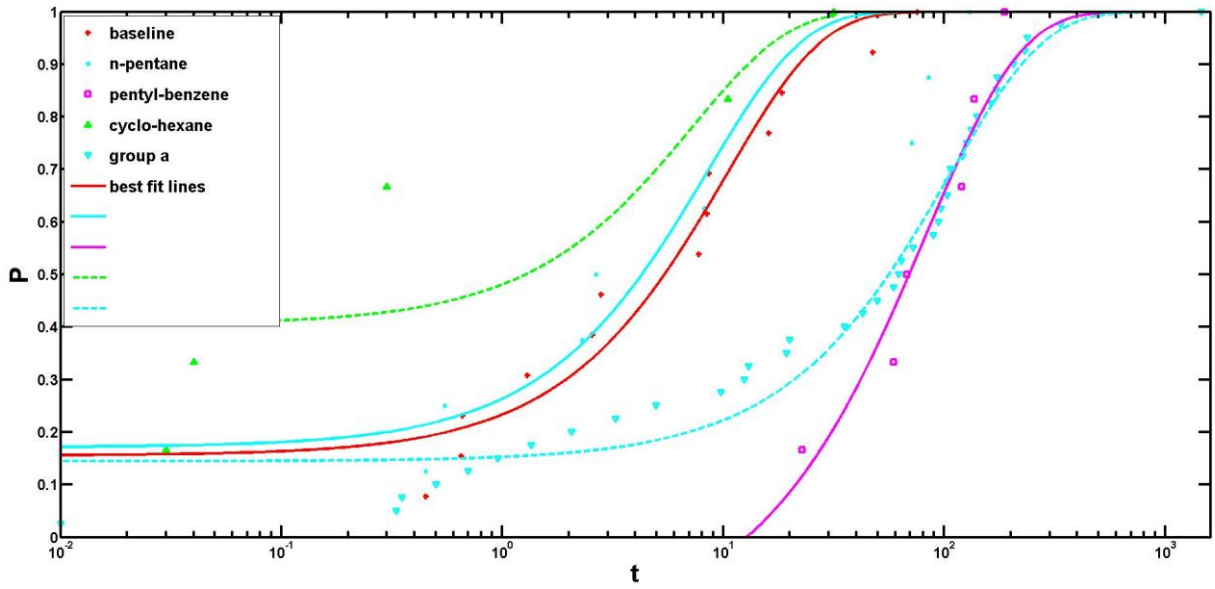

Fig. 10, $P - t_d$ plot 6 °C, 90 bar, with n-C_{6+} = n-hexane, n-octane, n-dodecane and pentyl-benzene

Variations of temperature and added volume of hydrocarbon liquids

All the experiments were carried out at an experimental pressure of 90 bar, a content of 50 ml distilled water and a cooling rate of 3 °C / h. The only things that were varied were the volume and type of added hydrocarbon liquid, and the static temperature of the experiments. An overview has been given in Table 2.

Cyclo-hexane experiments were carried out at both 6 °C and 8 °C, the result is shown in

Fig. 11. The result is according to the expectations in the same way as for the baseline series in Fig. 8. As we shall see later, there is a chance that cyclo-hexane is trigging formation of sII hydrate. In that case the subcooling would be much larger than for sI, at the experimental temperatures in question. This may be the explanation for the large τ-values for the series at 6 °C.

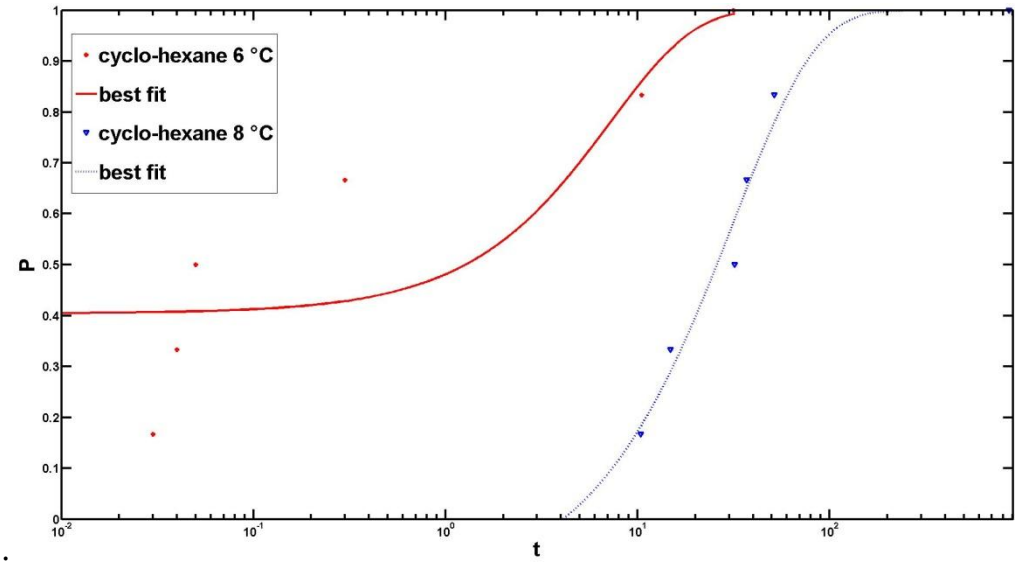

Fig. 11, $P - t_d$ plot 6 °C, 8 °C, 90 bar, additive = cyclo-hexane 2 ml

The variations of temperature in the case of n-octane additive show some peculiar effects, when compared to the expected pattern featured in Fig. 8. With an additive of 2 ml n-octane, and varying the temperature between 6 °C to 8 °C, the lowest temperature, 6 °C appears to give higher value of t_d than both 7 °C and 8 °C Fig. 12, while with additive = 6 ml n-octane (Fig. 13), the pattern appears reversed, but it still not following the expected pattern.

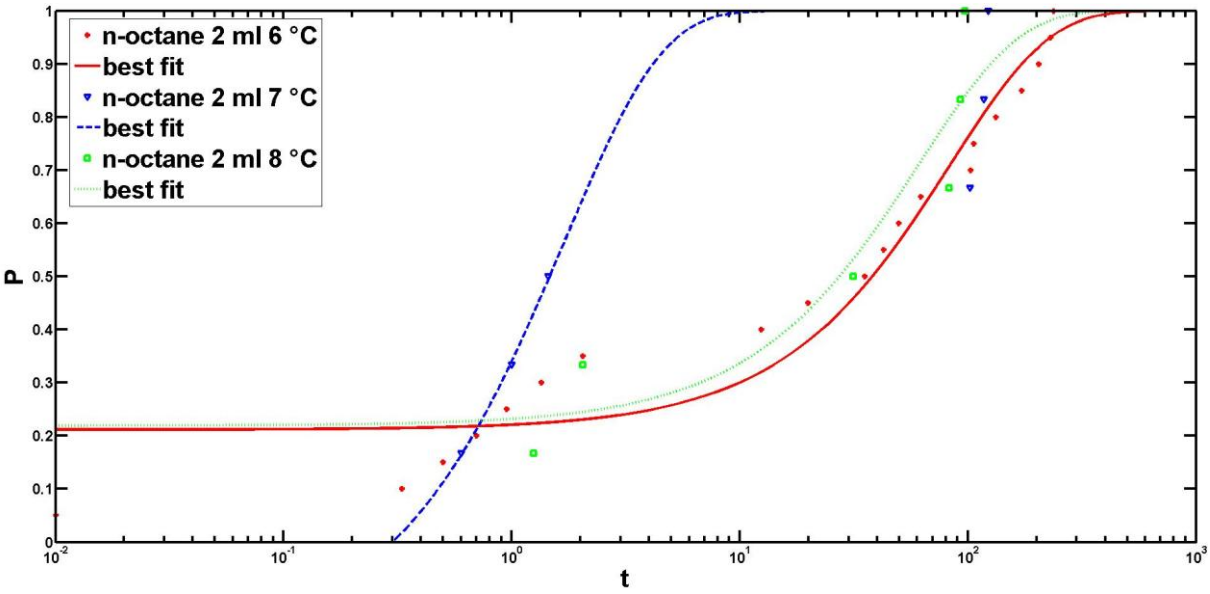

Fig. 12, $P - t_d$ plot 6-8 °C, 90 bar, additive = n-octane 2 ml

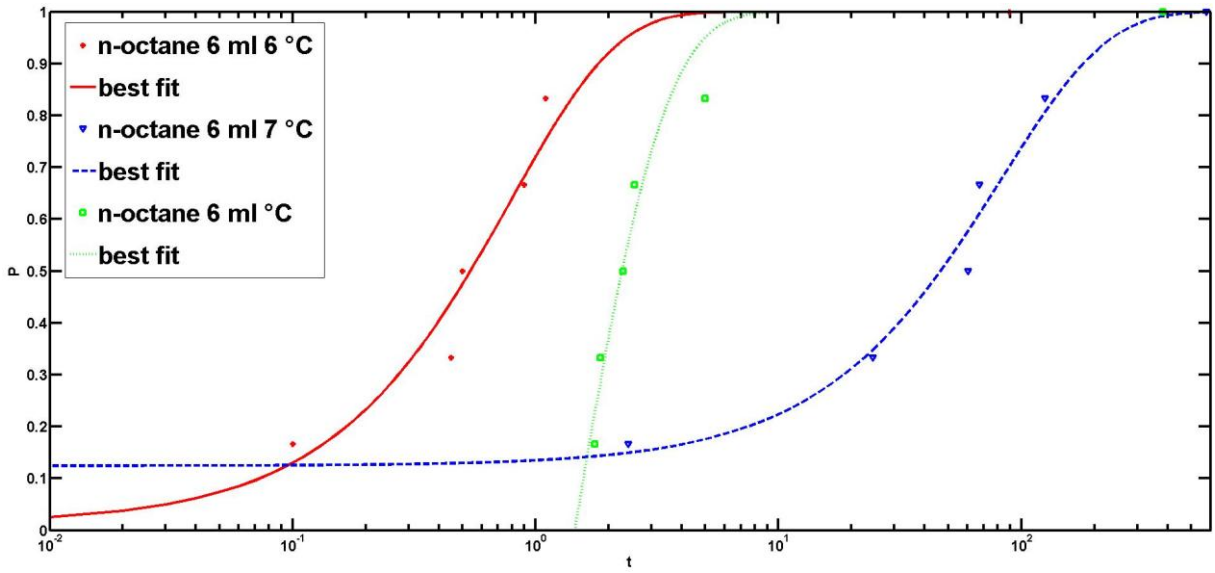

Fig. 13, $P - t_d$ plot 6-8 °C, 90 bar, additive = n-octane 6 ml

The variation of added amount of n-octane also apparently show a remarkable pattern, where the addition of 2 ml n-octane to the baseline system delay nucleation compared to baseline, while the addition of 6 ml n-octane seemingly speed up the nucleation process, Fig. 14. This apparent effect will be discussed later.

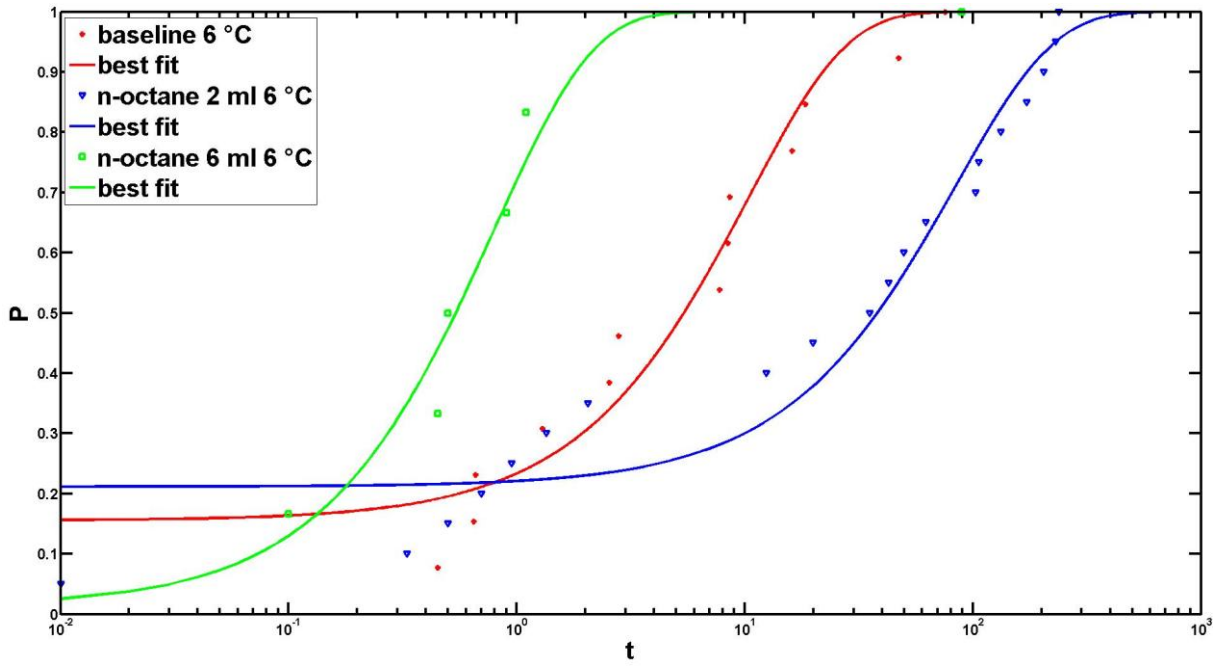

Fig. 14, $P - t_d$ plot 6 °C, 0 – 6 ml n-octane

Refused experiments

As explained in section "Experimental procedure", the starting point of the experiment was assumed to be after the cooling period, when the stirring was started. Therefore, at $t = 0$, the subcooling was already established and the system had in principle already been in metastable condition for some hours, but without stirring.

If evidence of hydrate formation was seen at $t < 0$, the experiment was refused. This was rarely the case, but it is known to happen from time to time [6].

Fig. 15 show an example of a refused experiment, cyclo-hexane 2 ml 8 °C, which is easily distinguished from the normal behavior depicted in Fig. 6. The sharp fall in pressure at Time = 125 is when stirring starts at $t \equiv 0$.

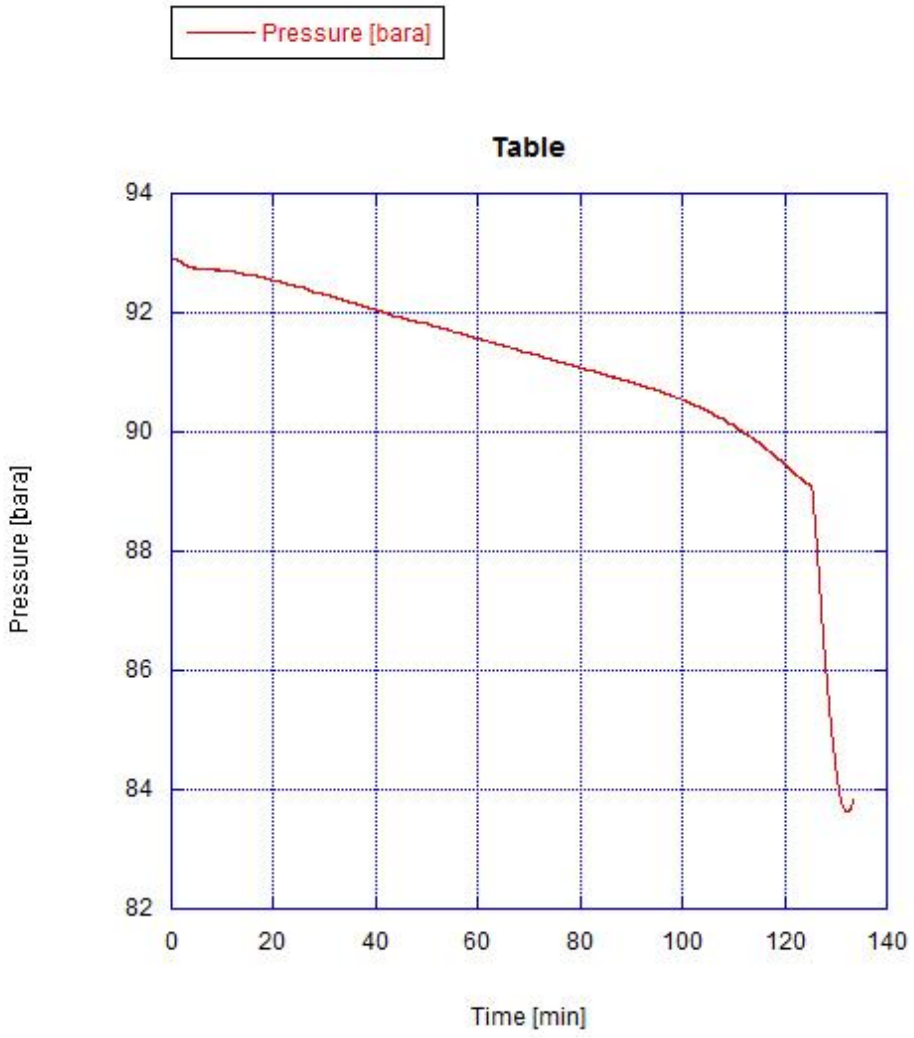

Fig. 15, refused experiment, cyclo-hexane 2 ml, 8 °C

Investigation of formed structure

In some of the experiments with cyclo-hexane additive it was noted that the pressure was significantly lower after the melting process succeeding a "finished" experiment, compared to the initial pressure before cooling (at initial temperature of 13.5 °C). Cyclo-hexane is known to stabilize the large cavities of sII hydrate, and this has an equilibrium temperature far above 13.5 °C at pressure around 90 bar [42].

Therefore it was made[1] a melting experiment of the methane cyclo-hexane system, where it was cooled under constant stirring from 21 °C to 8 °C, then slowly heated back to 21 °C. See Fig. 16 . It is especially interesting to note the deviation from the straight line at around 14 °C. This could indicate that sII is forming at that temperature. It is also interesting to note the different behavior of the supposed nucleation at 14 °C, to that of 11 °C. If both these events are nucleation, of sII and sI respectively, it indicates a great difference in kinetics of the nucleation regimes.

It is also interesting to note that even if the deviation from the straight line is present in all three repetitions, the sharp pressure drop of the second nucleation event is not occurring on identical temperatures, as could be expected if there were ice-like crystals already present in form of sII hydrate [17].

In any case, it can be seen that the melting curve (the lower of the two main lines of Fig. 16) is containing two distinct equilibrium events, which are assumed to be melting points of two different hydrate structures, sI at ca 14 °C and sII at ca 18.7 °C. Even if this is so, the equilibrium point of sI cannot be assumed to be increased around 1.8 °C, compared to pure sI methane hydrate at this temperature [10]. This is probably an apparent effect caused by a high rate of heating until around 17 °C. The temperature on the scale is measured in the gas phase, which was probably heated more efficiently due to lower heat capacity than that of water.

The equilibrium temperature at 18.7 °C is very close to the values reported for sII hydrate in cyclo-hexane – methane systems by Sun et al [42], and this is another strong indication of that we have sII hydrate in the system.

[1] These experiments were carried out by another student, Sjur Meling Eriksen

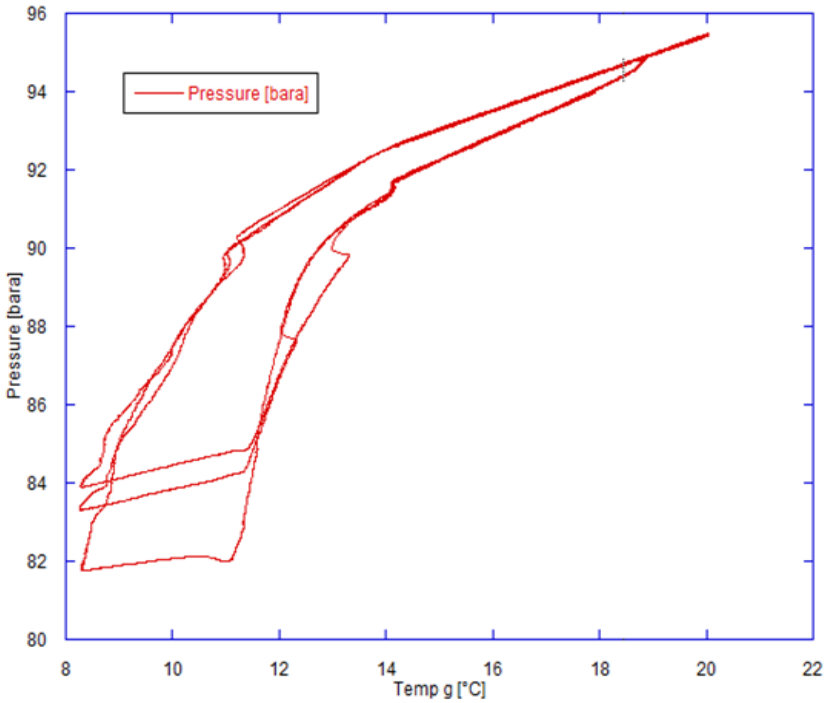

Fig. 16, melting experiment of methane – cyclo-hexane system

A similar melting point experiment was conducted for n-pentane, see Fig. 17. N-pentane is not reported to form stabilize hydrate with methane alone, but it can stabilize the largest cage of sH-hydrate if combined with f ex 2,2-dimethyl-butane [39]. This seem to be in accordance with our experiments.

There is, however, the same kind of deviation from linear $P - T$ behaviour as we see in the case of cyclo-hexane melting experiments, although occurring at a lower temperature. This is interesting and could indicate that the interpretation that the deviation in the case of cyclo-hexane is in fact not sII hydrate nycleation, but some other phenomenon.

This deviation behavior may at first sight resemble the case in Fig. 15, but it is a totally different case since there was constant stirring in the melting experiments of cyclo-hexane and n-pentane.

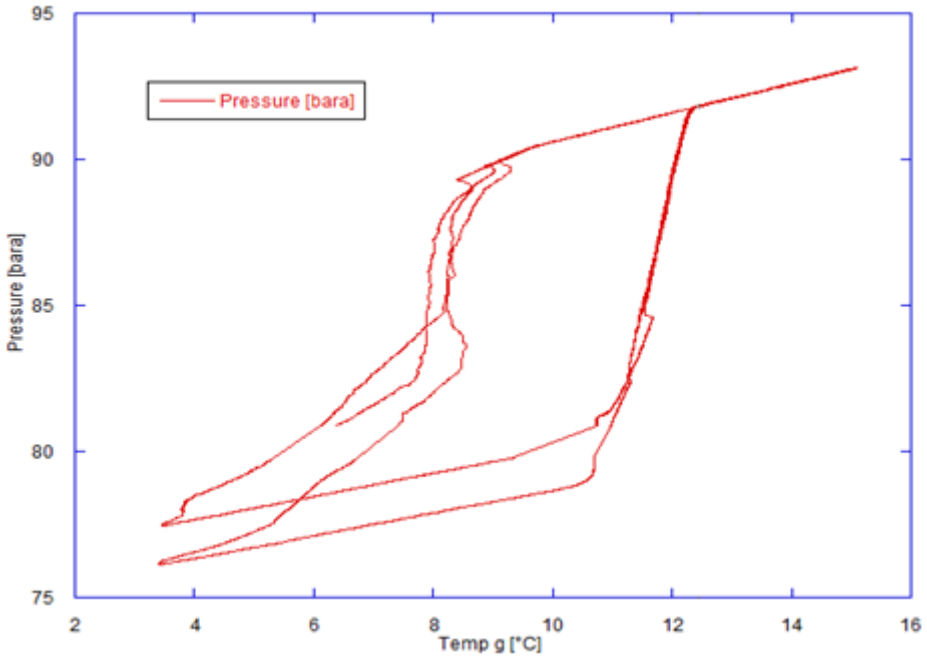

Fig. 17, melting experiment on n-pentane

Attempting to calculate the activation energy of methane hydrate

According to the theory of finding the activation energy through an Arrhenius plot based on Eq. (11), an attempt was made to calculate the activation energy of pure methane sI hydrate in binary methane – water system (baseline series). The data used in the calculation is presented in Table 3, and the Arrhenius plot is showed in Fig. 18.

Table 3, data for calculation of activation energy and critical radius of methane sI hydrate

$T\ [°C]$	$T\ [K]$	J	$\ln(J)$
6	279.15	0.09691	-2.3340
7	280.15	0.06684	-2.7055
8	281.15	0.01186	-4.4346

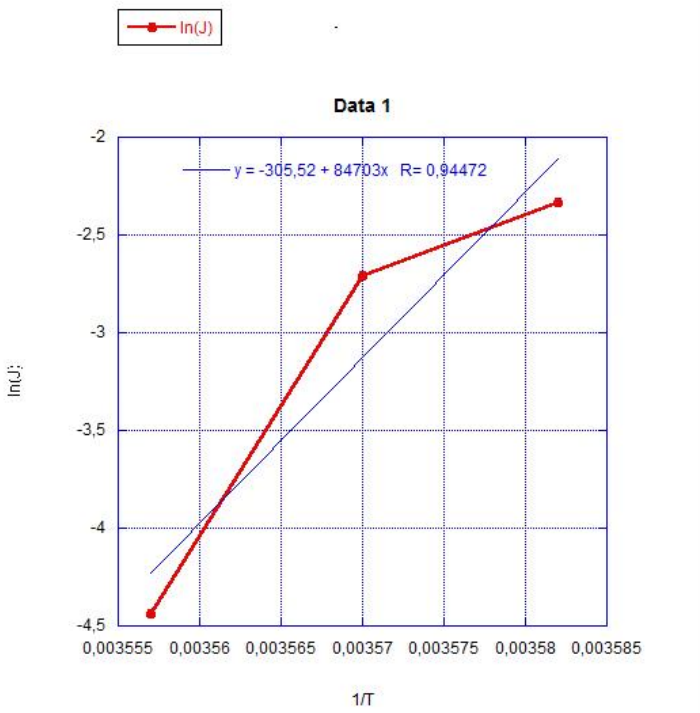

Fig. 18, Arrhenius plot, linear fit of $ln(J)$ vs $\frac{1}{T}$ for pure methane – water system

If then the interfacial tension of water – hydrate is assumed to be that of water – ice, $\sigma = 0.0276\, J/m^2$, and Bolzmann's constant $k_B = 1.38066 \times 10^{-23}\, J/K$ [36]

Then the activation energy $E_A = 84703 \times 1.38066 \times 10^{-23} = 1.17 \times 10^{-18} J$

Combined with Eq. (10) this gives $r_c = \sqrt{\frac{3 \times E_A}{4\pi\sigma}} = 31.8$Å

This is in the expected range of size, as Englezos et al [43] calculated the critical radius for methane hydrate to be in the range of 30 – 170 Å.

In theory, the same kind of calculation could probably have been done in the case of the n-octane series, but because of their poor agreement of nucleation time as a function of temperature, the result would probably not be meaningful.

Discussion

Metal activity effects on the experimental results?

In an attempt of explaining some of the unexpected results of the experiments carried out in this work, possible effects of the early repair of the cell was considered.

The autoclave was constructed of titanium, which is a chemically reactive material if the protective oxide layer is removed [44]. It was suspected that the apparent change in nucleation behavior may originate from the active titanium surface that was introduced through the grinding and scraping described in connection with the repair described in the previous section. Such active surface would oxidize over time and eventually become passive, and it may therefore be important to consider the chronology of the experiments and look for patterns that might support this hypothesis.

Overview of experimental series

The experimental work was made in the tradition of Svartås [6] and Abay [5], and typically sets of 6 – 8 repeated experiments were performed, if not unexpected results were encountered, which in such case called for more repetitions. Of the results presented earlier in this work, several series are therefore combined from shorter series carried out at different chronological occasions.

First, a detailed table of all experimental series shall be presented, where the chronology is represented by the days the experiments were executed. The repair of the stirring blade defines day 0, so that the first set (baseline pre-repair series) starts at day -10.

Of the series presented in Table 4, the series “baseline 6 °C” and “baseline 6 °C 2nd try” were later combined to the “baseline 6 °C” mentioned in previous sections. The same is the case for the three series of n-octane 2 ml 6 °C. **It is therefore important that the reader recognize the difference between the combined series and the individual sub-series presented only in this section.**

Table 4, chronological order of the experiments

Day	Set of experiments	Rate, J	Offset time, τ, min
-10 – -1	baseline pre-repair	0.01251	-20.38
0	repair of stirring blade		
2 – 4	baseline 1 (also referred to as "baseline 6 °C", or just "baseline")	0.3161	-0.4743
5 – 8	baseline 8 °C	0.01186	-12.45
10 – 15	n-hexane 2 ml 6 °C	0.005223	-23.44
15 – 18	n-octane 2 ml 6 °C (as referred to when mentioned above, f ex in Fig. 21.	0.006879	17.35
18 – 22	n-pentane 4 ml 6 °C	0.1182	-1.589
24 – 26	cyclo-hexane 2 ml 6 °C	0.1378	-3.759
27 – 33	pentyl-benzene 2 ml 6 °C	0.01228	12.71
34 – 39	n-dodecane 2 ml 6 °C	0.01248	-10.15
39 – 44	baseline 7 °C	0.06684	-2.365
42 – 46	cyclo-hexane 2 ml 8 °C	0.0319	4.092
44 – 50	iso-pentane 4 ml 6 °C	0.01522	-14.7
48 – 51	n-octane 6 ml 6 °C	1.261	-0.0104
52 – 54	n-octane 6 ml 8 °C	0.8468	1.45
66 – 67	n-octane 2 ml 8 °C	0.01627	-15.21
67 – 69	n-octane 2 ml 7 °C	0.5947	0.2996
69 – 73	n-octane 6 ml 7 °C	0.01205	-11.03
74 – 75	n-octane 2 ml 6 °C 2nd try	0.03057	-12.7
81 – 83	n-octane 2 ml 6 °C 3rd try (after changing araldite sealing on magnetic stirrer)	0.7053	0.4116
84 – 85	baseline 6 °C 2nd try (with pre-repair being try 0)	0.04738	-2.963

If one looks at the first three baseline series, Fig. 19, the results apparently show good accordance with theory. They show t_d - values that appear to be a function of temperature, regardless of chronology.

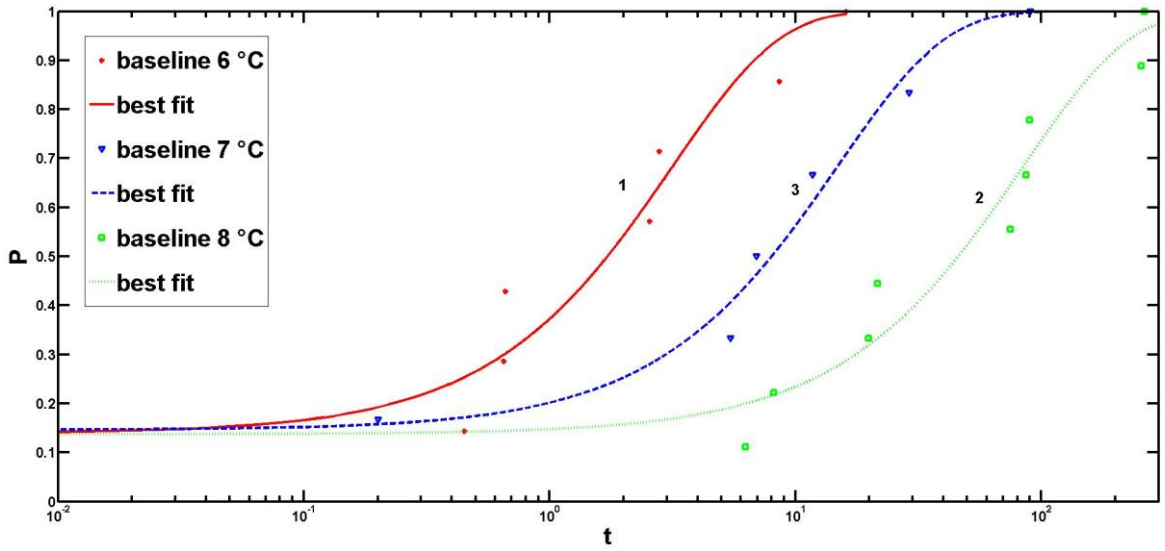

Fig. 19, baseline $P - t_d$, 6 °C, 7 °C, 8 °C, 90 bar, numbers in graph denote chronological order.

The n-octane 2 ml series of different temperatures,Fig. 20 , show an unexpected pattern, where the t_d - values of 6 °C are approximately two orders of magnitude longer than the t_d - values of the 7 °C series. Could it be that the chronology plays a part through the gradual passivation of the metal surface, and that the n-octane system is more sensitive to this effect than to temperature effects?

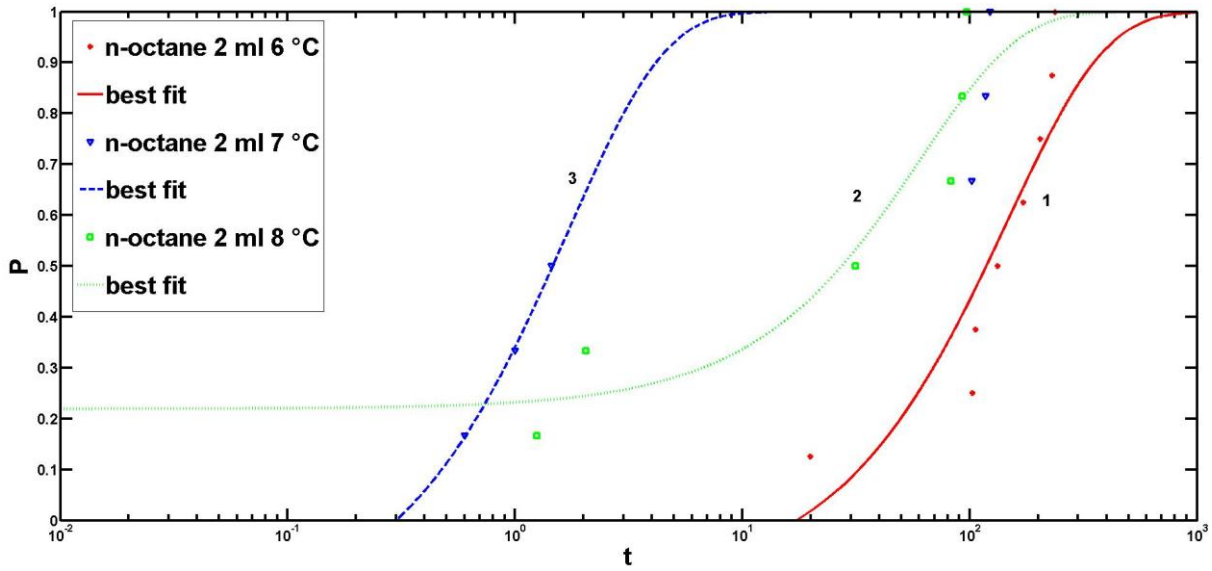

Fig. 20, $P - t_d$ plot 6-8 °C, 90 bar, additive = n-octane 2 ml, numbers in graph denote chronological order.

However, the chronology-dependence hypothesis does not hold when checking the case of n-octane 6 ml, different temperatures, Fig. 21. While these series do not show agreement with theory, in that 8 °C seemingly give shorter t_d - values than 7 °C, the chronological response is reversed compared to the sets of n-octane 2 ml additive.

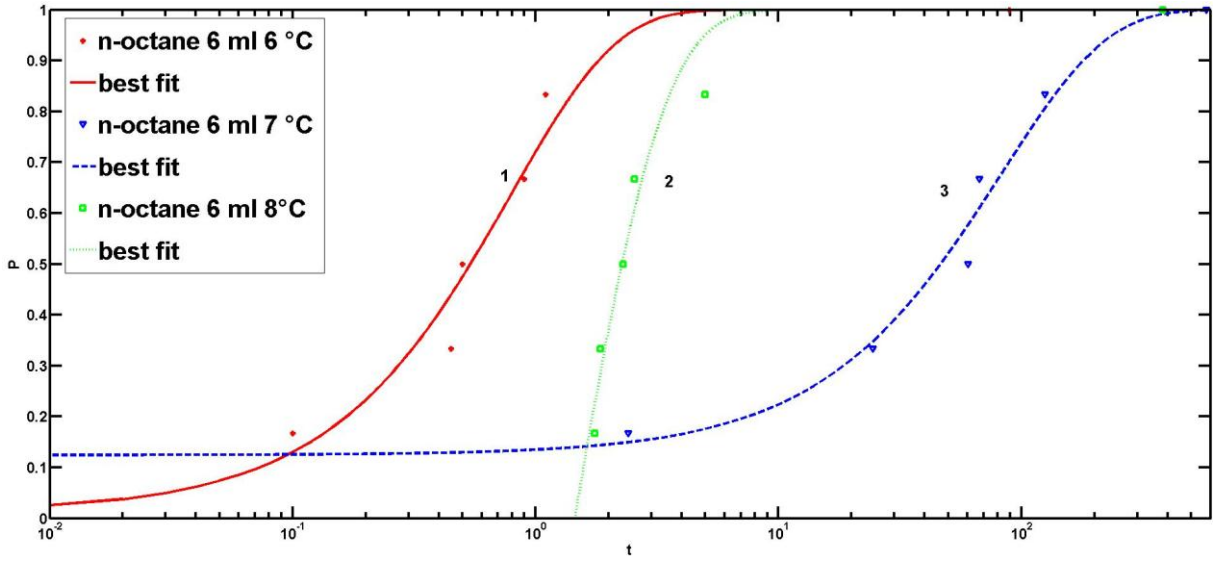

Fig. 21, $P - t_d$ plot 6-8 °C, 90 bar, additive = n-octane 6 ml, numbers in graph denote chronological order.

Too few experiments?

The method of trying to extract the supposedly inherent phenomenological properties of J and τ was initially developed by Toschev et al [20]. They explicitly state that in order to use this method with acceptable reliability, a "very large amount" of experiments needs to be carried out. They suggest 500 individual experiments per set in order to get reliable results of the highly stochastic phenomenon of crystallization. Furthermore, he also states that it is necessary to have a process where a single nucleation event can easily be detected, and this is clearly not the case with a hydrate nucleation process[1].

Another study utilizing the same method executed 80 tests per series while examining the nucleation of certain organic acids [23], though one team investigating hydrate nucleation did only 10 experiments per set.

When it comes to previous work done at the University of Stavanger, with very similar types of equipment that are used in this work, it has been the impression that titanium autoclaves give more stochastic test results than do similar equipment made of alloy steel. This have also been the case with methane nucleation systems, on which experiments seem to have been harder to repeat than if performed on systems with multi-component gas. [6]

[1] Toschev et al [20] did not work with hydrate crystallization, but with nucleation of metal salts from melt. However, their work is often cited when the method is used for examining hydrate nucleation processes.

Another example indicating that the "standard" number of experiments in this work has been too few is the case of n-octane 6 ml, 6 °C. Two series of six experiments each were performed in a close time interval, they are number 3 and 4 in Fig. 22 These series are made with exactly the same additives, the only possible difference between the two is that the magnet holder of the cell was sealed with new araldite to hold the magnets. On the plot of Fig. 22 looks probable that the experimental points are in fact part of the same probability distribution. The curve fitting analysis of the two series give very differentiating output: The value of J is more than 23 times higher on the "3rd try"-series than on the "2nd try" set, while the τ – value differs more than 13 minutes.

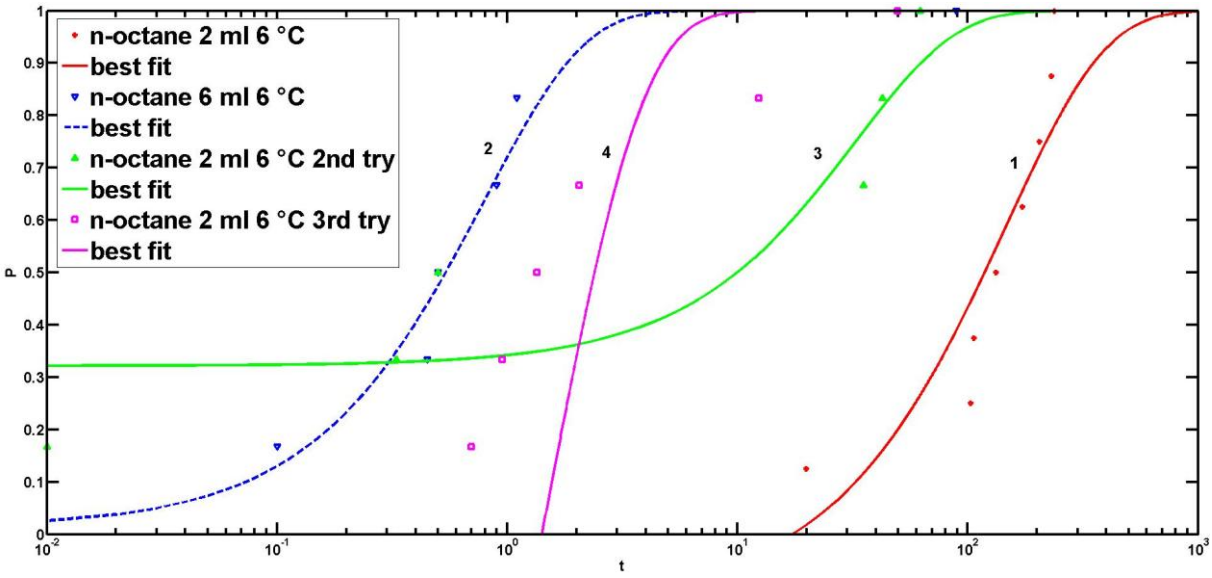

Fig. 22, n-octane, 2 ml and 6 ml, 6 °C

It then seems reasonable to conclude that the apparently unexplainable results obtained in this work may well be an effect of much too few experiments. Unfortunately, limited time has made it impossible to increase the number of experiments further.

On the original purpose of this work

Unfortunately, virtually no progress has been made to reveal the effect on methane hydrate nucleation of either LHC carbon number or interfacial tension against water. Both the components that did not delay nucleation had relatively low carbon number, cyclo-hexane and n-pentane. At least in the case of cyclo-hexane, it can be suspected that this in an effect of its ability to form sII together with methane. Because this has a much greater subcooling level at the experimental conditions, it must be regarded as another case entirely instead of being a catalyzing effect on the (sI-) nucleation of the water – methane system. Actually, most liquid hydrocarbon components appeared to have a delaying effect on the nucleation of methane

hydrats, in this work. The effect was also very much alike, whether it was iso-pentane, pentyl-benzene or n-dodecane.

Overall, the work has been dominated by unexpected results and the attempts to find out what lies behind this.

Critics on the experimental method

If it is assumed that the probability distribution function is correct, it is absolutely certain that we will never be able to measure the longest possible value of t_d. Nevertheless, we assume that we find exactly that, in every single series, because we set the probability of detecting nucleation at $t_{d,\,max} = 1$. Even if we know for certain that this is wrong. Surely, the analysis would benefit from assigning a more realistic P-value to the longest t_d found experimentally. Perhaps $P(t_{d,max}) = N/(N+1)$ and $P(t_{d,min}) = 1/(N+1)$, where $t_{d,min}$ is the shortest measured value and $t_{d,max}$ is the longest measured value in a series.

It should be a very doable task to write a code, for example in matlab, that generates a great amount of stochastic data series with the same probability distribution that we assume the hydrate nucleation to have. With such a program, it should also be easy to automatically try out different variations of the regression analysis done in this work to find a method which statistically estimates the most correct value of τ and J. In any case, it seems unlikely that using Eq. (8) gives the best result, as it assigns at least one P-value that we know is too high.

Furthermore, it seems appropriate to mention the plotting technique utilized in this work. Experimentally measured t_d - values are plotted against assigned P-values. The P values are not experimentally measured. This can actually make a series look like one, and vice versa. The effect is well illustrated in Fig. 9 and Fig. 10, where the exact same data is presented either as one series or as several individual series, where the probability points seem to be scattered over a much larger area.

On the Arrhenius plot method to calculate the activation energy

It can probably work satisfactory in many cases, but there may be a problem when liquid hydrocarbons are added to the system, because these will prefer to form a thin film on the aqueous surface. This film is very thin and will likely be saturated with hydrate stabilizing gas molecules. When agitating the system, this film will be entering the water phase and thus greatly increase the surface where heterogeneous nucleation may occur.

But because the interfacial tension between the liquid hydrocarbon phase and water is sensitive to temperature alterations, the “effective area” of the gas saturated film entering the water bulk may be affected in a way that can make the result from an Arrhenius plot

calculation less reliable. The Arrhenius plot rely on the assumption of unaltered area, or effective area, where heterogeneous nucleation can take place.

The τ –variable

The offset time τ, which is an output of the regression analysis made in this and other works [5, 23, 24], seems to have a little theoretical foundation. Usually, it is given a brief explanation that it represents the time between the formation of the first stable nuclei (which is at the saddle point ΔG_{crit} of Fig. 3) until "the time when it can be macroscopically detected". It is further said that this is possible because the system usually is in a metastable state long before the formal "start" of the experiment.

However, this approach have at least two weak points. The first is that the size of a (sub-critical) hydrate cluster fluctuate extremely rapidly, it can be born, grow and be redissolved in a time scale of nano-seconds [6, 17]. Now, if the nucleus can reach nanometer-size in nano-seconds, it seems very unlikely that it should not reach macroscopic size in the time-scale of seconds. What mechanism could slow the growth process so dramatically after it has reached critical size? Indeed, Sloan and Koh write that (based on molecular dynamic simulation) "the initial nucleus, on reaching a critical size, expands rapidly resulting in the entire system freezing"[17].

It is sometimes argued that we don't have agitation in the metastable period before the start of an experiment, and therefore a stable nucleus may remain undetected for a long time. If this is true, it is definitely a problem to superimpose the same "time lag" also to nucleation events which have rather long detection times (t_d - values). Indeed, it is a significant logical dilemma that the "period of non-detection" is regarded to be the same whether it lies in the nucleation regime before agitation starts, after agitation starts, or lies in both regimes. It should at least be considered to be shorter, or neglible, after the start of stirring, due to the great impact that agitation has on nucleation kinetics.

It is also interesting to note that Natarayan et al [18] conclude from physical observations (of turbidity) that it is unlikely with a long growth period where the nuclei remain undetectable. Furthermore, they report that when nucleation is detected, a very large amount of nuclei appear at the same time. This synchronized appearance of a large amount of nuclei, though on stochastic time, seem to be a paradox to which I have seen no comment during this work. In any case, it seems to be inconsistent with the probability-distribution assumed in this work, as this explicitly assumes nucleation as single, independent events. It may of course still be that

the very first nucleation event is independent and stochastic, but that this then starts a chain reaction of non-independent events.

Conclusion

The experimental results indicate that most of the investigated hydrocarbon liquid components delay formation of methane sI hydrate formation, virtually with the same effect, even to the point that they may be grouped together.

Two components seem to make an exception: n-pentane, which seem to have little effect, if any, and cyclo-hexane, which seem to have a propagating effect. The effect of cyclo-hexane is probably not an effect that can be related to baseline at all, since it has been concluded from melting experiments that cyclo-hexane may and do form sII hydrate under experimental conditions.

The critical radius of methane hydrate system was calculated, and it was 31,8 Å, which is in in the lower part of the expected lengt scale.

The computational results of this work must unfortunately be regarded as generally unreliable, because a large part of the results is qualitatively in disagreement with commonly accepted theory. The poor reliability is probably due to statistical analysis of too little experimental data where the nature of the investigated phenomenon, methane hydrate nucleation, is highly stochastic.

During the experimental work, a novel method of detecting hydrate nucleation was successfully used. The small but characteristic pressure pulse preceeding catastrophic growth seem to be a fast, easy and reliable way of detecting hydrate nucleation.

Future Research

The deviation from linear $P - T$ behavior during cooling and stirring of n-pentane and cyclo-hexane system (Fig. 16 and Fig. 17) seems to be a distinct feature that is hard to explain, and it deserves further investigation.

The possible effect of "fresh" (active) titanium metal surface compared to oxidized inactive surface would also be interesting to study experimentally, if not else to rule it out as a possible error factor when using titanium autoclaves for hydrate nucleation experiments.

Matlab simulation of large amounts of synthetic data resembling experiments could be an interesting way of finding a more effective and accurate analysis regression method.

1. Hammerschmidt, E.G., *Formation of Gas Hydrates in Natural Gas Transmission Lines.* Industrial & Engineering Chemistry, 1934. **26**(8): p. 851-855.
2. Sloan, E.D. and C.A. Koh, *Clathrate hydrates of natural gases*, in *Chemical Industries*, J.G. Speight, Editor. 2008, CRC Press: Boca Raton, Fla. p. 1 - 29.
3. Tohidi, B., *Gas Hydrates: Friend or Foe?* 2005.
4. Kelland, M.A., *History of the Development of Low Dosage Hydrate Inhibitors.* Energy & Fuels, 2006. **20**(3): p. 825-847.
5. Abay, H.K., *Kinetics of gas hydrate nucleation and growth*, 2011, UiS: Stavanger.
6. Svartås, T.M.,Jan 2012 - June 2012.
7. Mehta, A.P. and E.D. Sloan, *Structure H hydrate phase equilibria of methane + liquid hydrocarbon mixtures.* Journal of Chemical & Engineering Data, 1993. **38**(4): p. 580-582.
8. Davies, S.R., K.C. Hester, J.W. Lachance, C.A. Koh, and E. Dendy Sloan, *Studies of hydrate nucleation with high pressure differential scanning calorimetry.* Chemical Engineering Science, 2009. **64**(2): p. 370-375.
9. Kashchiev, D. and A. Firoozabadi, *Nucleation of gas hydrates.* Journal of Crystal Growth, 2002. **243**(3–4): p. 476-489.
10. Sloan, E.D. and C.A. Koh, *Clathrate hydrates of natural gases*, in *Chemical Industries*, J.G. Speight, Editor. 2008, CRC Press: Boca Raton, Fla. p. 319 - 536.
11. Mooijer-van den Heuvel, M.M., C.J. Peters, and J. de Swaan Arons, *Influence of water-insoluble organic components on the gas hydrate equilibrium conditions of methane.* Fluid Phase Equilibria, 2000. **172**(1): p. 73-91.
12. Jufu, F., L. Buqiang, and W. Zihao, *Estimation of fluid-fluid interfacial tensions of multicomponent mixtures.* Chemical Engineering Science, 1986. **41**(10): p. 2673-2679.
13. Ragil, K., D. Bonn, D. Broseta, J. Indekeu, F. Kalaydjian, and J. Meunier, *The wetting behavior of alkanes on water.* Journal of Petroleum Science and Engineering, 1998. **20**(3–4): p. 177-183.
14. Aspenes, G., S. Høiland, T. Barth, and K.M. Askvik, *The influence of petroleum acids and solid surface energy on pipeline wettability in relation to hydrate deposition.* Journal of Colloid and Interface Science, 2009. **333**(2): p. 533-539.
15. Nordbø, T., *Effects of HC liquids on Point of Spontaneous Nucleation and the growth of structure I*

methane hydrate, in *Department of Petroleum Engineering*2011, University of Stavanger: Stavanger.
16. Haddad, W.M., V. Chellaboina, and S.G. Nersesov, *Thermodynamics: a dynamical systems approach*. 2005, Princeton: Princeton University Press. xii, 187 s.
17. Sloan, E.D. and C.A. Koh, *Clathrate hydrates of natural gases*, in *Chemical Industries*, J.G. Speight, Editor. 2008, CRC Press: Boca Raton, Fla. p. 113 - 181.
18. Natarajan, V., P.R. Bishnoi, and N. Kalogerakis, *Induction phenomena in gas hydrate nucleation.* Chemical Engineering Science, 1994. **49**(13): p. 2075-2087.
19. Kashchiev, D., *Nucleation: basic theory with applications*. 2000, Butterworth Heinemann: Boston. p. 231 - 273.
20. Toschev, S., A. Milchev, and S. Stoyanov, *On some probabilistic aspects of the nucleation process.* Journal of Crystal Growth, 1972. **13–14**(0): p. 123-127.

21. Kashchiev, D., *Nucleation: basic theory with applications*. 2000, Butterworth Heinemann: Boston. p. 413 - 427.
22. Tegze, G., T. Pusztai, G. Toth, L. Granasy, A. Svandal, T. Buanes, T. Kuznetsova, and B. Kvamme, *Multiscale approach to CO[sub 2] hydrate formation in aqueous solution: Phase field theory and molecular dynamics. Nucleation and growth.* The Journal of Chemical Physics, 2006. **124**(23): p. 234710.
23. Jiang, S. and J.H. ter Horst, *Crystal Nucleation Rates from Probability Distributions of Induction Times.* Crystal Growth & Design, 2010. **11**(1): p. 256-261.
24. Takeya, S., A. Hori, T. Hondoh, and T. Uchida, *Freezing-Memory Effect of Water on Nucleation of CO2 Hydrate Crystals.* The Journal of Physical Chemistry B, 2000. **104**(17): p. 4164-4168.
25. Buchanan, P., A.K. Soper, H. Thompson, R.E. Westacott, J.L. Creek, G. Hobson, and C.A. Koh, *Search for memory effects in methane hydrate: Structure of water before hydrate formation and after hydrate decomposition.* The Journal of Chemical Physics, 2005. **123**(16): p. 164507.
26. Skovborg, P. and P. Rasmussen, *A mass transport limited model for the growth of methane and ethane gas hydrates.* Chemical Engineering Science, 1994. **49**(8): p. 1131-1143.
27. Asserson, R.B., A.C. Hoffmann, S. Høiland, and K.M. Asvik, *Interfacial tension measurement of freon hydrates by droplet deposition and contact angle measurements.* Journal of Petroleum Science and Engineering, 2009. **68**(3–4): p. 209-217.
28. Volmer, M. and A. Weber, *Keimbildung in übersättigten Gebilden.* Zeitschrift für Physikalische Chemie, 1926. **119**.
29. Firoozabadi, A.F. and H.J.R. JR., *Surface Tension Of Water-Hydrocarbon Systems At Reservoir Conditions.* Journal of Canadian Petroleum Technology, 1988. **27**(3).
30. Sun, C.-Y., G.-J. Chen, and L.-Y. Yang, *Interfacial Tension of Methane + Water with Surfactant near the Hydrate Formation Conditions.* Journal of Chemical & Engineering Data, 2004. **49**(4): p. 1023-1025.
31. Matsubara, H., M. Murase, Y.H. Mori, and A. Nagashima, *Measurement of the surface tensions and the interfacial tensions of <i>n -pentane-water and R 113-water systems.* International Journal of Thermophysics, 1988. **9**(3): p. 409-424.
32. Jasper, J.J., M. Nakonecznyj, C.S. Swingley, and H.K. Livingston, *Interfacial tensions against water of some C10-C15 hydrocarbons with aromatic or cycloaliphatic rings.* The Journal of Physical Chemistry, 1970. **74**(7): p. 1535-1539.
33. Zeppieri, S., J. Rodríguez, and A.L. López de Ramos, *Interfacial Tension of Alkane + Water Systems†.* Journal of Chemical & Engineering Data, 2001. **46**(5): p. 1086-1088.
34. Kashchiev, D., *Nucleation: basic theory with applications*. 2000, Butterworth Heinemann: Boston. p. 116 - 135.
35. Zatsepina, O.Y. and B.A. Buffett, *Nucleation of CO2-hydrate in a porous medium.* Fluid Phase Equilibria, 2002. **200**(2): p. 263-275.
36. Schmitt, E.A., D. Law, and G.G.Z. Zhang, *Nucleation and crystallization kinetics of hydrated amorphous lactose above the glass transition temperature.* Journal of Pharmaceutical Sciences, 1999. **88**(3): p. 291-296.
37. Kashchiev, D., *Nucleation: basic theory with applications*. 2000, Butterworth Heinemann: Boston. p. 17 - 44.
38. Sloan, E.D. and C.A. Koh, *Clathrate hydrates of natural gases*, in *Chemical Industries*, J.G. Speight, Editor. 2008, CRC Press: Boca Raton, Fla. p. 45 - 102.

39. Lee, J.-w., H. Lu, I.L. Moudrakovski, C.I. Ratcliffe, and J.A. Ripmeester, *n-Pentane and n-Hexane as Coguests in Structure-H Hydrates in Mixtures of 2,2-Dimethylbutane and Methane.* Angewandte Chemie International Edition, 2006. **45**(15): p. 2456-2459.
40. Walsh, M.R., C.A. Koh, E.D. Sloan, A.K. Sum, and D.T. Wu, *Microsecond Simulations of Spontaneous Methane Hydrate Nucleation and Growth.* Science, 2009. **326**(5956): p. 1095-1098.
41. Vysniauskas, A. and P.R. Bishnoi, *A kinetic study of methane hydrate formation.* Chemical Engineering Science, 1983. **38**(7): p. 1061-1072.
42. Sun, Z.-G., S.-S. Fan, K.-H. Guo, L. Shi, Y.-K. Guo, and R.-Z. Wang, *Gas Hydrate Phase Equilibrium Data of Cyclohexane and Cyclopentane.* Journal of Chemical & Engineering Data, 2002. **47**(2): p. 313-315.
43. Englezos, P., N. Kalogerakis, P.D. Dholabhai, and P.R. Bishnoi, *Kinetics of formation of methane and ethane gas hydrates.* Chemical Engineering Science, 1987. **42**(11): p. 2647-2658.
44. Bearinger, J.P., C.A. Orme, and J.L. Gilbert, *In situ imaging and impedance measurements of titanium surfaces using AFM and SPIS.* Biomaterials, 2003. **24**(11): p. 1837-1852.